Craniofacial ontogeny in mosasauridae

Amelia R Zietlow Corresp. 1

1 Department of Biology, Carthage College, Kenosha, Wisconsin, United States

Corresponding Author: Amelia R Zietlow
Email address: azietlow@carthage.edu

Mosasaurs were large aquatic lizards that lived during the Late Cretaceous. Their fossils are found across the globe, but despite a multitude of specimens of varying maturity, a detailed growth series has not been proposed for any mosasaur taxon. Four taxa – *Tylosaurus proriger, T. kansasensis/nepaeolicus, Tethysaurus nopcsai,* and *Mosasaurus hoffmannii* – have robust fossil records with specimens spanning a wide range of sizes and are thus ideal for studying mosasaur ontogeny. Furthermore, an analysis of growth provides an opportunity to test the synonymy of *T. kansasensis* with *T. nepaeolicus,* sexual dimorphism, anagenesis, heterochrony, and, by sampling several mosasaur taxa, identification of ancestral patterns of mosasaur growth. Fifty-nine hypothetical growth characters were identified, including size-dependent, size-independent, and phylogenetic characters, and quantitative cladistic analysis was used to recover growth series for the four taxa. The results supported the synonymy of *T. kansasensis* with *T. nepaeolicus* and that *T. kansasensis* represent juveniles of *T. nepaeolicus*. A Spearman rank-order correlation test resulted in a significant correlation between two measures of size (total skull length and quadrate height) and maturity for all taxa except *M. hoffmannii*, which is likely due to the small sample size and limited data available for the taxon. A novel hypothesis of anagenesis in Western Interior Seaway *Tylosaurus* species, driven by peramorphy, is proposed here. Finally, 17 growth changes – seven of which involve the quadrate – were shared across two or more taxa and none of the ontogram topologies showed evidence of skeletal sexual dimorphism.

Craniofacial Ontogeny in Mosasauridae

Amelia R. Zietlow[1]

[1] Department of Biology, Carthage College, Kenosha, Wisconsin, U.S.A.

Corresponding Author:
Amelia R. Zietlow[1]
2001 Alford Park Drive, Kenosha, WI, 53140, U.S.A
Email address: azietlow@carthage.edu

Abstract

Mosasaurs were large aquatic lizards that lived during the Late Cretaceous. Their fossils are found across the globe, but despite a multitude of specimens of varying maturity, a detailed growth series has not been proposed for any mosasaur taxon. Four taxa – *Tylosaurus proriger, T. kansasensis/nepaeolicus, Tethysaurus nopcsai,* and *Mosasaurus hoffmannii* – have robust fossil records with specimens spanning a wide range of sizes and are thus ideal for studying mosasaur ontogeny. Furthermore, an analysis of growth provides an opportunity to test the synonymy of *T. kansasensis* with *T. nepaeolicus,* sexual dimorphism, anagenesis, heterochrony, and, by sampling several mosasaur taxa, identification of ancestral patterns of mosasaur growth. Fifty-nine hypothetical growth characters were identified, including size-dependent, size-independent, and phylogenetic characters, and quantitative cladistic analysis was used to recover growth series for the four taxa. The results supported the synonymy of *T. kansasensis* with *T. nepaeolicus* and that *T. kansasensis* represent juveniles of *T. nepaeolicus*. A Spearman rank-order correlation test resulted in a significant correlation between two measures of size (total skull length and quadrate height) and maturity for all taxa except *M. hoffmannii*, which is likely due to the small sample size and limited data available for the taxon. A novel hypothesis of anagenesis in Western Interior Seaway *Tylosaurus* species, driven by peramorphy, is proposed here. Finally, 17 growth changes – seven of which involve the quadrate – were shared across two or more taxa and none of the ontogram topologies showed evidence of skeletal sexual dimorphism.

Introduction

Literature Review

Mosasaur ontogeny. The first published study of growth in mosasaurs was done by Caldwell (1996), which sought to determine the patterns of ossification in the autopodial skeleton across mosasaurs and to test the congruence between these growth processes and mosasaur phylogeny

(Caldwell, 1996). The main result found that few ossified carpals is the ancestral condition, whereas more derived species have progressively more ossified carpals (Caldwell, 1996). Also, a low number of carpals is characteristic of juveniles (Caldwell, 1996).

In 2007, Caldwell published on the growth and replacement of mosasaur teeth. Rather than focusing on a specific taxon, he provided a clade level eight stage model of tooth replacement in mosasaurs based on data from several taxa and proposed that the rooted teeth of mosasaurs arose independently of other thecodont animals (Caldwell, 2007). However, the study makes no mention of growth-related differences in mosasaur dentition.

Also in 2007, Pellegrini published the first study of osteohistology in mosasaur limb bones. By counting lines of arrested growth, he found that mosasaur growth was initially fast, and then slowed when they reached five to seven years old; he noted that the rate of growth is faster overall than extant terrestrial squamates (Pellegrini, 2007). The decrease in growth rate is interpreted as the onset of sexual maturity, given that five to seven years is also the onset of sexual maturity in large extant varanid lizards (Pellegrini, 2007). However, no proxies for maturity beyond chronological age were explicitly given.

In 2012, Houssaye and Tafforeau examined vertebral microanatomy to test the hypothesis that juvenile mosasaurs inhabited shallower environments than adults; in other marine reptiles, an ontogenetic shift from shallow habitats to deeper ones was inferred through progressive loss of bone mass (Wiffen et al., 1995). The authors acknowledged that the assessment of maturity is based on size alone, given that skeletochronology is not reliable in mosasaur vertebrae due to a high amount of inner bone resorption (Houssaye and Tafforeau, 2012). They found that vertebral microstructure is similar between juveniles and adults, which implies that juveniles were as agile swimmers as adults and, therefore, the authors reject the hypothesis that juvenile mosasaurs were restricted to shallow, sheltered nurseries (Houssaye and Tafforeau, 2012). They also note that, relative to other squamates, mosasaur vertebrae seem to be paedomorphic in that there is a general inhibition of bone remodeling (Houssaye and Tafforeau, 2012).

In 2017, Carpenter described the vertebral morphology of several specimens of *Tylosaurus proriger*, including a purported juvenile, RMM 5610. The goal was to deduce the method of swimming of this species by analyzing the degree of vertebral mobility (Carpenter, 2017). In addition to providing evidence that adult *T. proriger* were carangiform swimmers (propulsion generated by movement of the hips and tail), differences were seen in the vertebral mobility of RMM 5610, suggesting a faster, tail-driven method of swimming in juveniles (Carpenter, 2017).

In 2018, Green published a growth series of four specimens of *Clidastes* sp. that was based on histological data. The author concluded that the growth rate in *Clidastes* was rapid during its first year of life, moderate between the second and sixth years, and slow from the seventh year onward; based on growth rates, it was hypothesized that mosasaurs were ectothermic (Green, 2018). These results are similar to those of Pellegrini (2007); however, like the earlier study, these results are limited by a small sample size (number of specimens) and he did not provide any estimates of maturity beyond size and chronological age.

***Tylosaurus proriger*.** *T. proriger* was a particularly large mosasaur – the largest individual, the "Bunker" specimen (KUVP 5033), has an estimated total skull length (TSL) of 1.7 m (Table 1) – that lived in the Western Interior Seaway (WIS) during the upper Santonian to the middle Campanian, between 84 and 78 million years ago (Ma) (Jiménez-Huidobro and Caldwell, 2019). The type specimen of *T. proriger* (MCZ 4374) was described by Cope in 1869 and includes a partial snout, cranial fragments, and thirteen vertebrae (Russell, 1967). Cope originally named the species *Macrosaurus proriger*. The genus was changed by Leidy to *Tylosaurus* in 1873, of which *T. proriger* is the type species (Leidy, 1873; Everhart, 2017).

T. proriger is an unquestionably valid taxon diagnosed by the following cranial characters: (1) premaxilla-maxilla suture ends posterior to the fourth maxillary tooth; (2) quadrate suprastapedial process reaches half the length of the complete bone; (3) quadrate infrastapedial process is moderately developed; (4) quadrate tympanic ala is thin; (5) medial crest of the frontal is well-developed; (6) prefrontal overlaps the postorbitofrontal; (7) dorsal, medial, and lateral invasion of the parietal by frontal alae; and (8) teeth that lack flutes (Russell, 1967; Jiménez-Huidobro and Caldwell, 2019).

A description of the smallest known *Tylosaurus* specimen (FHSM VP 14845) was published by Konishi, Jiménez-Huidobro, and Caldwell (2018). Although it is not identifiable to species, it shares many features with *Tylosaurus* generally, especially with the juvenile *T. proriger* specimen, RMM 5610 (Konishi, Jiménez-Huidobro, and Caldwell, 2018). The authors determined that the specimen is most likely a neonate (newborn) using an estimated total body length and neonate-to-maternal body length proportion data from extant varanid lizards (Konishi, Jiménez-Huidobro, and Caldwell, 2018). Also, the authors rejected the possibility that the length of the premaxillary predental rostrum is sexually dimorphic due to its presence in this extremely young individual, but they did note that it is much shorter than what is seen in adult specimens (Konishi, Jiménez-Huidobro, and Caldwell, 2018).

Also in 2018, Stewart and Mallon described two purported subadult specimens of *T. proriger* and hypothesized the growth pattern of various skull structures. The study revealed a significant correlation of all individual bone measurements with TSL, as well as isometric growth for all characters except quadrate height, which was found to be positively allometric, and premaxillary predental rostrum length, which was found to be negatively allometric (Stewart and Mallon, 2018).

***Tylosaurus kansasensis* and *Tylosaurus nepaeolicus*.** *T. kansasensis* and *T. nepaeolicus* are both known from the WIS during the upper Coniacian to the lower Santonian, from 88 to 85 Ma (Everhart, 2017; Jiménez-Huidobro and Caldwell, 2019). The type specimen of *T. nepaeolicus* (AMNH FARB 1565) was described by Cope in 1874 and includes a quadrate, jaw fragments, rib fragment, and single dorsal vertebra (Russell, 1967; Jiménez-Huidobro, Simões, and Caldwell, 2016). The type specimen of *T. kansasensis* (FHSM VP 2295) was

described by Everhart in 2005 and consists of an articulated skull and six associated cervical vertebrae.

T. nepaeolicus is diagnosed by the following cranial characters: (1) premaxilla-maxilla suture ends posteriorly above midpoint between third and fourth maxillary teeth; (2) prefrontal overlaps the postorbitofrontal; (3) frontal with dorsal midline crest poorly developed or absent in adult; (4) lateral borders of parietal table slightly convex; (5) ectopterygoid does not contact the maxilla; (6) infrastapedial process of quadrate poorly developed or absent; (7) suprastapedial process of quadrate reaches half the length of the complete bone; (8) tympanic ala thick; (9) mandibular condyle of the quadrate mediolaterally broad; and (10) lateral crest of tympanic ala ends posteriorly near mandibular condyle (Jiménez-Huidobro and Caldwell, 2019).

T. kansasensis is diagnosed by the following cranial characters: (1) premaxilla rostral foramina large; (2) infrastapedial process of quadrate poorly developed or absent; (3) medial ridge of quadrate diverges ventrally; (4) frontal with dorsal midline crest that is high, thin, and well-developed; (5) medial sutural flanges of frontal large, extend long distance onto parietal; (6) parietal foramen adjacent to or invading frontal-parietal suture; (7) dorsal postorbitofrontal with low rounded transverse edge; (8) posteroventral angle of jugal is 90 degrees; (9) ectopterygoid does not contact maxilla; (10) quadrate suprastapedial process without constriction; (11) quadrate ala thick; (12) alar concavity of quadrate shallow (Everhart, 2005).

In 2016, Jiménez-Huidobro, Simões, and Caldwell proposed that specimens of *T. kansasensis* (Everhart, 2005) represent juveniles of *T. nepaeolicus*. They identified several characters in *T. kansasensis* that purportedly show the juvenile conditions seen in *T. proriger* and concluded that there are "no differences between the two nominal species that cannot be attributed to size, and thus ontogenetic stage" (Jiménez-Huidobro, Simões, and Caldwell, 2016:80), and that *T. kansasensis* are therefore juveniles of *T. nepaeolicus*. Also, the authors suggested that *T. proriger* may be paedomorphic relative to *T. nepaeolicus* due to the presence of a dorsal midline crest on the frontal, a feature purportedly seen in *T. kansasensis*, but not *T. nepaeolicus* (Jiménez-Huidobro, Simões, and Caldwell, 2016). The authors provided no justification (or references to one) for identifying one *T. proriger* specimen, RMM 5610, as a juvenile, and all others (e.g., AMNH FARB 4909) as adults. The following characters were proposed to be ontogenetically variable: definition of the parietal nuchal fossa; medial curvature of the quadrate suprastapedial process; thickness of the quadrate suprastapedial process; thickness of the frontal posterolateral processes; and presence of the frontal dorsal midline crest (Jiménez-Huidobro, Simões, and Caldwell, 2016). Despite identifying these characters, the authors do not propose a growth series.

In 2018, Stewart and Mallon rejected the hypothesis of Jiménez-Huidobro, Simões, and Caldwell (2016) that *T. kansasensis* represent juveniles of *T. nepaeolicus*, stating that the growth trends between *T. kansasensis* and *T. nepaeolicus* do not match what is seen in *T. proriger*, and that there is not enough evidence to support the proposed ontogenetic characters (Jiménez-Huidobro, Simões, and Caldwell, 2016; Stewart and Mallon, 2018).

Tethysaurus nopcsai. *Te. nopcsai* is a small, basal russelosaurine (the lineage that includes *Tylosaurus*; see Fig. 1) from Morocco that lived during the Turonian, from 94 to 90 Ma during a transgression of the Atlantic Ocean (Bardet, Suberbiola, and Jalil, 2003; Simões et al., 2017). The type specimen (MNHN GOU 1) was described by Bardet, Suberbiola, and Jalil in 2003 and is represented by a nearly complete skull.

Te. nopcsai is diagnosed by the following cranial characters: (1) prefrontal strongly vaulted in anterior view; (2) parietal with triangular table ending posteriorly in two pointed pegs overlying the supraoccipital; (3) jugal with a large and wide ascending ramus; (4) medullar floor of the basioccipital pierced by three foramina; (5) splenial with a large notched dorsomedial process; (6) surangular exposed medially ventral to the coronoid; (7) 19 to 20 maxillary teeth; (8) 15 to 19 pterygoid teeth; and (9) at least 19 dentary teeth (Bardet, Suberbiola, and Jalil, 2003). Ten years after the taxon was named, Houssaye and Bardet (2013) described two juvenile specimens of *Te. nopcsai* (MNHN GOU 4 and MNHN GOU 5) that were found in the same site as the type specimen. The specimens are considered juveniles (but not embryos) based on their small size, poor ossification of articular surfaces, and histological data. The authors estimate the skull length of MNHN GOU 4 to have been less than 100 mm, and the total body length to have been less than 3 m.

Mosasaurus hoffmannii. *M. hoffmannii* lived in the Maastrichtian, from 72 to 66 Ma, and it is known from the WIS and several locations bordering the Atlantic Ocean, including the eastern coast of the United States, western Africa, many localities across Europe, and western Russia (Street and Caldwell, 2017). This taxon was especially large; the smallest individual in this project, IRSNB R 12, has a TSL of 880 mm, which is bigger than the largest *T. nepaeolicus*, and the largest specimen, PRM 2546/CCMGE 10/2469 (*M. hoffmannii*), rivals the largest *T. proriger* – it too has an estimated TSL of 1.7 m (Grigoriev, 2014; Table 1). *M. hoffmannii* was named in 1829 by Mantell, but the type specimen of *M. hoffmannii* and *Mosasaurus* (MNHN AC 9648) had already been described by Cuvier in 1808 and consists of a nearly complete skull (Lingham-Soliar, 1995; Street and Caldwell, 2017).

M. hoffmannii is diagnosed by the following cranial characters: (1) quadrate tympanic rim with additional anteroventral corner; (2) 13 maxillary teeth; (3) 14 dentary teeth; and (4) 8 pterygoid teeth (Street and Caldwell, 2017).

Very little work has been done on growth in *M. hoffmannii*. For example, although Lingham-Soliar (1995) described the morphology and functional anatomy of *M. hoffmannii* in great detail, the paper makes no mention of ontogenetic variation. *M. hoffmannii* was included in the studies of autopodial skeleton ossification and tooth replacement by Caldwell in 1996 and 2007, respectively, but those studies focused on mosasaurs as a group rather than any particular taxon. In 1999, Mulder proposed that *M. maximus* – found along the east coast of the United States – and *M. hoffmannii* – found in western Africa, Russia, and across Europe – are a single, transatlantic taxon based on many morphological similarities; ontogenetic variation is mentioned

with respect to the shape and robustness of the premaxillary rostrum, but it is not explicitly used to support synonymy of *M. maximus* with *M. hoffmannii*.

In 2015, Harrell and Martin described an *M. hoffmannii* specimen (TLAM NH.HR.2009.032.0001) found in South Dakota, which significantly extended the geographic range of the taxon farther north in the WIS. In addition to a description of the skull, the authors found evidence to support the synonymy of *M. hoffmannii* and *M. maximus* that was first proposed by Mulder (1999). They also identified several ontogenetically variable characters, including the shape of the frontal in dorsal view, dentary depth, and the shape of a notch on the anterolateral flange of the coronoid; the abstract mentions that the shape of the supratemporal fenestrae also varies with maturity, but this is not mentioned anywhere else in the article. The authors provided growth series that showed the growth changes associated with frontal shape and the anterolateral notch of the coronoid, but they are limited to three and four specimens, respectively (Harrell and Martin, 2015). Although variation in the quadrate is noted, they did not consider it to be ontogenetic.

Assessment. Overall, there is a deficit of literature devoted to growth in any individual mosasaur taxon, and despite the several papers that do address growth in mosasaurs, the topic remains poorly understood. Little to no justification beyond size or histological data is given for determining the relative maturity of specimens, and growth stages are limited to the vague categories of 'juvenile,' 'subadult,' and 'adult.' No study has attempted to combine all types of data – size, proportional, and size-independent – using an objective, quantifiable, and replicable method to recover a growth series for mosasaurid species. In addition to enhancing our understanding of mosasaur ontogeny, such an analysis could prove particularly useful in resolving the validity of certain species (in this case, *T. kansasensis*) and the presence or absence of sexual dimorphism.

Project Goals

The goals of this project were to use quantitative cladistic analysis to (1) recover the growth series of *T. proriger, T. kansasensis/nepaeolicus, Te. nopcsai,* and *M. hoffmannii*; (2) test whether total skull length (TSL) or quadrate height (QH) are appropriate proxies for relative maturity in these taxa; (3) test for sexual dimorphism in these taxa; (4) test the hypothesis that *T. kansasensis* represent juveniles of *T. nepaeolicus* (Jiménez-Huidobro, Simões, and Caldwell, 2016)*;* (5) test the hypothesis the presence of a frontal midline crest in *T. proriger* is paedomorphic relative to *T. nepaeolicus* (Jiménez-Huidobro, Simões, and Caldwell, 2016); (6) test for anagenesis in *Tylosaurus* species that inhabited the WIS; (7) provide revised cranial diagnoses of *T. proriger* and *T. nepaeolicus/kansasensis* within an ontogenetic context (Bhullar, 2012); and (8) identify conserved patterns of growth in mosasaurs.

Materials & Methods

Quantitative Cladistic Analysis

Size-independent assessment of maturity. In fossil taxa, it can be difficult to discern whether morphologically similar, but differently sized, individuals are different species or different growth stages of a single species (Rozhdestvensky, 1965; Brinkman, 1988; Carr, 1999). In 1988, Brinkman suggested the identification of size-independent ontogenetically variable characters to resolve this problem. This does not mean that size is completely uninformative, just that size alone is not enough to accurately assess the relative maturities of individuals because it is possible for individuals of different maturities to be the same size and for individuals of the same maturity to be different sizes (Brinkman, 1988; Carr, 1999).

Cladistic analysis of growth. Ontogeny, like evolution, consists of a hierarchical accumulation of changes over time (Brochu, 1996). Thus, in the same way that the evolutionary relationships between taxa are recovered, cladistic analysis can be used to identify the relative maturity of specimens drawn from a sample of a single species (Brochu, 1996). This method allows size and size-independent data to be combined to recover a high-resolution growth series that is more precise than simply grouping multiple individuals into imprecise sets such as 'juveniles,' 'subadults,' and 'adults' (Fig. 2).

Separate character matrices were compiled for each taxon (except *T. kansasensis*/*nepaeolicus*; Data S1, S2, S3, S4). FHSM VP 14845, which is only identifiable to *Tylosaurus* sp., was included in both *Tylosaurus* datasets given it was found between the two species stratigraphically and could be referable to either taxon (Konishi, Jiménez-Huidobro, and Caldwell, 2018). Character states with the juvenile condition were coded with zeroes and increasingly mature states were coded with progressively higher numbers. Multistate characters were coded for characters that are not binary (three or more states), and all characters were run unordered. A hypothetical embryo, coded with all zeroes, was added as the analogue of the outgroup in each dataset to polarize the characters, since an embryo expresses the least mature condition of all character states (Brochu, 1996; Carr and Williamson, 2004; Frederickson and Tumarkin-Deratzian, 2014). Following the method of Carr and Williamson (2004) and Frederickson and Tumarkin-Deratzian (2014), an artificial adult was added *a posteriori* to identify the most mature specimen of each taxon; should the analysis with the artificial adult fail to recover a single most mature specimen, the individual specimen with the most growth changes – i.e., with the greatest number of unambiguously optimized synontomorphies (shared growth characters) – was considered the most mature (Fig. 3).

Compilation and analysis of the data matrices. Hypothetical growth characters were identified and coded using literature descriptions and measurements, as well as first-hand observation of fossils at the Field Museum of Natural History (Chicago, IL), Fryxell Geology Museum (Rock Island, IL), American Museum of Natural History (New York, NY), Sternberg Museum of Natural History (Hays, KS), and Kansas University (Lawrence, KS). Character sources are summarized in Table S1 and measurements and tooth counts are listed in Tables 1

and 2, respectively. Across all taxa, a total of fifty-nine characters were identified, which includes two measures of size (TSL and QH), seven proportional characters, 19 size-independent characters, and 30 phylogenetic characters (Data S5; see Fig. S1 for exemplars of select morphological characters and their states). Of the phylogenetic characters, 11 could not be identified with certainty by the author (A. R. Z.) in any taxon (noted in Data S5), and so while they are included in the data matrices and the character list, they were excluded from all of the analyses; codes for those characters are from the literature.

Size characters, including proportional character calculations, were rounded to the nearest whole number. Most phylogenetic character states were numbered as they are in Bell (1997), and ontogenetic characters were numbered according to literature descriptions or naïvely according to patterns uncovered in this project (i.e., the state seen in mostly small individuals was coded as the less developed state and the state seen in mostly larger individuals was coded as the more developed state). Data matrices were compiled in Mesquite (Maddison and Maddison, 2018) and analyzed in TNT (Goloboff and Catalano, 2016) using new technology and traditional searches, and in PAUP (Swofford, 2003) using exhaustive (*Te. nopcsai* and *M. hoffmannii*) and branch-and-bound (*T. proriger, T. kansasensis/nepaeolicus*, all three *Tylosaurus* taxa) searches, respectively; exhaustive searches in PAUP could not be used for the *Tylosaurus* matrices because of the large (greater than 12) number of specimens.

This project makes use of data drawn from 106 specimens housed in several North American institutions, as well as one in Japan, five in Europe, and two in Russia (Table 3 and Table S1); of those, 47 were studied first-hand; all others were coded from descriptions and measurements in the literature, and photographs online or in the primary literature (sources for coding specimens are listed in Table S1). The total numbers of specimens coded for each taxon are as follows: 5 *Tylosaurus* sp.; 39 *T. proriger*; 21 *T. kansasensis*; 14 *T. nepaeolicus*; 5 *Te. nopcsai*; and 22 *M. hoffmannii*. Several specimens of each taxon were removed from the final analyses due to incomplete or redundant coding (Table 3), and any characters that were not coded for more than a single specimen were excluded from the analyses.

Testing Congruence Between Size and Maturity

Size alone is often not a reliable indicator of relative maturity (Rozhdestvensky, 1965; Brinkman, 1988; Brochu, 1996; Carr, 1999). To test this hypothesis in mosasaurs, once the growth series were recovered, the congruence between size and maturity in each taxon was tested using the method of Frederickson and Tumarkin-Deratzian (2014), where the growth stages and TSL measurements for each specimen were converted into ranks (Tables 4, 5, 6, 7, 8) and then analyzed in SPSS (IBM Corp., 2019) using a Spearman rank-order correlation test. If size and maturity are congruent, the correlation will be positive and statistically significant ($p < 0.05$). Because mosasaur skulls are not always complete enough for an accurate measurement or estimate of TSL, the same method was used to test the congruence between QH and maturity. The normality of the growth ranks, size ranks, and measurement data were tested using a Shapiro-Wilk test.

Testing Sexual Dimorphism and Taxon Validity

The ontogram recovered by a cladistic analysis can be used to test for the presence of sexual dimorphism (Frederickson and Tumarkin-Deratzian, 2014). If no evidence for sexual dimorphism is recovered, the ontogram will be linear (Fig. 4A). If, however, sexual dimorphism is present, the ontogram will bifurcate (i.e., a single node will have two groups of multiple specimens) into two groups of specimens, corresponding to each sex, after one or more juvenile stages (Fig. 4B, C). It is also possible that the ontogram is linear and sexual dimorphism is instead recovered as two homologous sets of individual variations (Fig. 4D).

The growth series will also be used to test the validity of specimens assigned to each taxon. If specimens assigned to the taxon actually represent two or more different species, the ontogram will bifurcate into two or more groups (Fig. 4B, C) or it will be linear and recover two or more groups defined by shared sets of individual variations (Fig. 4D).

Test of synonymy between *T. kansasensis* and *T. nepaeolicus*. To test the hypothesis that *T. kansasensis* are juveniles of *T. nepaeolicus*, a single matrix including specimens of both taxa was constructed. This is not the first study that has used quantitative cladistic analysis to test a hypothesis regarding synonymy; Longrich and Field (2012) used the same approach to test, and reject, the hypothesis that specimens of the genus *Torosaurus* represent adults of another genus of North American horned dinosaur, *Triceratops*. Summaries of potential results are shown in Figure 5.

Test of Heterochrony in *Tylosaurus*

The hypothesis that the frontal dorsal midline crest of *T. proriger* is paedomorphic relative to *T. nepaeolicus* was tested by comparing the growth patterns for that trait across all four taxa in this project. If the presence of the frontal dorsal midline crest in *T. proriger* is paedomorphic relative to *T. nepaeolicus*, then it will be present in all *T. proriger* specimens, present in juvenile *T. nepaeolicus*, *Te. nopcsai*, and *M. hoffmannii*, and absent in mature *T. nepaeolicus*, *Te. nopcsai*, and *M. hoffmannii*.

Test of Anagenesis in *Tylosaurus*

Anagenesis – evolution within a single lineage (i.e., without branching into multiple new clades) over time – has been studied in several nonavian dinosaur taxa as a mechanism for producing species diversity, particularly in ceratopsians and tyrannosaurs (Horner, Varricchio, and Goodwin, 1992; Scanella et al., 2014; Carr et al., 2017; Wilson, Ryan, and Evans, 2020). In order for anagenesis to be defensible, the taxa in question must meet the following criteria: (1) they do not overlap stratigraphically; (2) they have a close phylogenetic relationship; (3) some specimens have intermediate morphology; and (4) they inhabited the same location (Carr et al., 2017; Wilson, Ryan, and Evans, 2020).

No previous study has proposed anagenesis as a mechanism of speciation in mosasaurs. Because of the large sample size and potential for high-resolution growth series, they are an ideal taxon for testing hypotheses of evolutionary processes, particularly anagenesis (Carr et al., 2017). In this project, the novel hypothesis that the *Tylosaurus* of the WIS are a single, anagenetic lineage will be tested. The three *Tylosaurus* species meet each criterion for anagenesis outlined above: (1) *T. kansasensis/nepaeolicus* and *T. proriger* do not overlap stratigraphically; (2) they are sister taxa (Jiménez-Huidobro and Caldwell, 2019); (3) some specimens have intermediate morphology (e.g., the quadrate infrastapedial process is absent or weak in *T. kansasensis* and *T. nepaeolicus*, and it is always present and well-developed in *T. proriger*); and (4) they all lived in the WIS.

If the cladistic analysis of growth based on the dataset including specimens of *T. kansasensis* and *T. nepaeolicus* supports their synonymy, then a single data matrix including specimens of all three taxa (i.e., *T. kansasensis/nepaeolicus* and *T. proriger*) will be compiled and analyzed; one the other hand, if the growth series of *T. kansasensis* and *T. nepaeolicus* suggests that they are two distinct species, then two matrices – one with *T. kansasensis* and *T. proriger*, and the other with *T. nepaeolicus* and *T. proriger* – will be constructed. If the hypothesis of anagenesis is supported, and speciation in WIS *Tylosaurus* was driven by peramorphy (extension or acceleration of growth), then the ontogram will show a progression from *T. kansasensis/nepaeolicus* to *T. proriger*, and if speciation was driven by paedomorphy (truncation or deceleration of growth), the ontogram will either show a progression from *T. proriger* to *T. nepaeolicus* or a progression from *T. kansasensis/nepaeolicus* to *T. proriger* that includes many character reversals; if anagenesis is not supported, specimens of both taxa will be interspersed with one another on the ontogram or the ontogram will bifurcate basally.

Furthermore, testing for anagenesis using ontogenetic data allows for another hypothesis to be tested: heterochrony as a driver of evolution in mosasaurs. Heterochrony is differences in the timing of developmental events (i.e., the developmental consequences of a truncation, extension, acceleration, or deceleration of growth in one taxon relative to another) (Reilly, Wiley, and Meinhardt, 1997) that produce the morphological differences between a descendent taxon from its ancestor. If heterochrony is an evolutionary mechanism in *Tylosaurus*, and the *Tylosaurus* species of the WIS are a single anagenetic lineage, then a cladistic analysis of growth will recover the specific developmental changes that produced *T. proriger* – the descendent – from *T. kansasensis/nepaeolicus* – the ancestor.

Results

Growth Series of *T. proriger*

A branch-and-bound search recovered one ontogram with a length of 83 steps, consistency index (CI) of 0.65, homoplasy index (HI) of 0.35, retention index (RI) of 0.76, and rescaled consistency index (RC) of 0.49 (Fig. 6). The topology was tested using a Bremer decay index approach, and resolution was lost after the addition of one step. A total of 17 growth stages were

identified; the analysis with the artificial adult and all 23 specimens did not recover a single most mature specimen, but a second analysis with the artificial adult which only included the eight most mature specimens (i.e., those with the most growth changes: KUVP 50090, KUVP 1032, ROM 7906, GSM 1, AMNH FARB 221, FMNH P15144, FHSM VP 3, and AMNH FARB 1555) identified FHSM VP 3 as the most mature individual. Character states that were unambiguously optimized as individual variation are listed in Table S2. The following growth stages are recovered:

Stage 1. This stage is not unambiguously defined by any character states (exemplar: *Tylosaurus* sp. neonate FHSM VP 14845).

Stage 2. The QH is between 50 and 99 mm and the mandibular condyle of the quadrate is completely ossified (exemplar: CMN 51258-51263).

Stage 3. The quadrate tympanic ala is thick (exemplar: AMNH FARB 1592).

Stage 4. The quadrate alar concavity is shallow (exemplar: FMNH UR902).

Stage 5. The occipital condyle is completely ossified (exemplar: AMNH FARB 2160).

Stage 6. The foramina on the premaxillary rostrum are small (exemplar: RMM 5610).

Stage 7. The premaxilla-maxilla suture is m-shaped and the mandibular condyle of the quadrate is rounded (exemplar: KUVP 66129).

Stage 8. The infrastapedial process of the quadrate is rounded (exemplar: CMN 8162).

Stage 9. The QH is greater than or equal to 13% TSL and the dentary is deep (exemplars: AMNH FARB 4909, KUVP 28705, KUVP 1033, and TMP 1982.050.0010). At this stage, the exemplar specimens share a distance between the first and sixth dentary teeth that is less than or equal to 23% TSL and less than or equal to 35% dentary length; KUVP 28705, KUVP 1033, and TMP 1982.050.0010 share a reversal to foramina on the premaxillary rostrum that are large and frontal medial suture flanges that are large; and KUVP 1033 and TMP 1982.050.0010 share a TSL that is between 800 – 999 mm.

Stage 10. The frontal posterolateral processes are thick and the dorsal ridge on the predental process of the dentary is present (exemplars: USNM 6086 and USNM 8898).

Stage 11. This stage is diagnosed by a TSL that is between 1000 – 1499 mm, a QH that is between 150 – 199 mm, and a dentary length that is less than or equal to 55% lower jaw length (exemplar: FFHM 1997-10).

Stage 12. The premaxillary rostrum is distinctly knobbed (exemplar: KUVP 50090).

Stage 13. The distance between the first and sixth dentary teeth that is less than or equal to 23% TSL (exemplar: KUVP 1032).

Stage 14. The quadrate suprastapedial process is thick (exemplars: ROM 7906, GSM 1, and AMNH FARB 221). At the stage, the exemplar specimens share a distance between the first and sixth maxillary teeth that is greater than or equal to 25% TSL and a reversal to a QH between 100 – 149 mm.

Stage 15. The distance between the first and sixth dentary teeth that is less than or equal to 35% dentary length, dentary length is between 60 – 56% lower jaw length, and the coronoid posteroventral process is present and fan-like (exemplar: FMNH P15144).

Stage 16. This stage is not unambiguously defined by any character states (exemplar: AMNH FARB 1555).

Stage 17 This stage is diagnosed by a reversal to a quadrate alar concavity that is deep (exemplar: FHSM VP 3).

Growth Series of *T. kansasensis* and *T. nepaeolicus*

A branch-and-bound search recovered one ontogram with a length of 90 steps, a CI of 0.59, an HI of 0.41, an RI of 0.62, and an RC of 0.36 (Fig. 7). The tree topology was tested using a Bremer decay index approach; resolution was lost after the addition of one step. A total of 12 growth stages were identified; the analysis with the artificial adult and all 19 specimens recovered YPM 3970 and FHSM VP 2209 as the most mature individuals. Notably, although the holotype of *T. nepaeolicus* is recovered as more mature (stage 9) than the holotype of *T. kansasensis* (stage 8), there are no unambiguously optimized synontomorphies that distinguish them (Fig. 7). Character states that were unambiguously optimized as individual variation are listed in Table S2. The following growth stages are recovered:

Stage 1. This stage is not unambiguously defined by any character states (exemplar: *Tylosaurus* sp. neonate FHSM VP 14845).

Stage 2. This stage is not unambiguously defined by any character states (exemplar: *T. kansasensis* FHSM VP 17206).

475
476 **Stage 3.** The premaxilla-maxilla suture is u-shaped (exemplars: *T. kansasensis* FHSM VP 9350
477 and *T. kansasensis* FHSM VP 2495). At this stage, the exemplar specimens share a deep dentary.
478
479 **Stage 4.** The foramina on the premaxillary rostrum are small and the quadrate mandibular
480 condyle is rounded (exemplar: *T. kansasensis* FHSM VP 78).
481
482 **Stage 5.** The QH is greater than or equal to 13% TSL, the quadrate ala rim is defined, and the
483 dorsal ridge on the predental process of the dentary is present (exemplar: *T. kansasensis* FHSM
484 VP 15632).
485
486 **Stage 6.** The QH is between 50 – 99 mm, the quadrate mandibular condyle is completely
487 ossified, and the basioccipital is reniform (exemplar: *T. kansasensis* FHSM VP 3366, *T.*
488 *kansasensis* FHSM VP 18520, and *T. nepaeolicus* FHSM VP 7262). At this stage, the exemplar
489 specimens share a decrease in dentary teeth (from 13 to 12).
490
491 **Stage 7.** The foramina on the premaxillary rostrum reverse from small to large (exemplar: *T.*
492 *kansasensis* FHSM VP 15631).
493
494 **Stage 8.** The posteroventral angle of the jugal is obtuse and the coronoid posteroventral process
495 is present as a bump (exemplar: *T. kansasensis* holotype FHSM VP 2295).
496
497 **Stage 9.** This stage is not unambiguously defined by any character states (exemplar: *T.*
498 *nepaeolicus* holotype AMNH FARB 1565).
499
500 **Stage 10.** The quadrate suprastapedial process is thick and the coronoid anterolateral notch is
501 present and shallow (exemplars: *T. kansasensis* FMNH PR2103, *T. kansasensis* FGM V 43, and
502 *T. nepaeolicus* AMNH FARB 2167). At this stage, the exemplar specimens share a quadrate
503 suprastapedial process that is not curved medially, and FGM V 43 and AMNH FARB 2167 share
504 a quadrate suprastapedial process that is long.
505
506 **Stage 11.** The premaxillary rostrum is distinctly knobbed, the frontal posterolateral processes
507 are thick, and there is an increase in dentary teeth (from 13 to 14) (exemplar: *T. nepaeolicus*
508 YPM 3974 and *T. nepaeolicus* AMNH FARB 124/134). At this stage, the exemplar specimens
509 share an absence of the parietal nuchal fossa and a distance between the first and sixth dentary
510 teeth that is greater than 35% dentary length.
511
512 **Stage 12.** This stage is diagnosed by a QH that is between 100 – 149 mm (exemplars: *T.*
513 *nepaeolicus* YPM 3970 and *T. nepaeolicus* FHSM VP 2209).
514

Analysis Including *T. kansasensis*, *T. nepaeolicus*, and *T. proriger*

Because the synonymy of *T. kansasensis* and *T. nepaeolicus* is supported, a data matrix including all three *Tylosaurus* taxa was analyzed (Data S6). A branch-and-bound search recovered 18 most parsimonious trees each with a length of 148 steps, a CI of 0.41, an HI of 0.59, an RI of 0.60, and an RC of 0.24 (Fig. 8). The tree topology was tested using a Bremer decay index approach; resolution was lost after the addition of one step. The analysis with the artificial adult and all 30 specimens did not recover a single most mature individual, but it did identify the group of adult *T. proriger* as more mature than the group of *T. nepaeolicus*; a second analysis, which only included the five most mature individuals (as recovered by the individual analysis of *T. proriger*; FMNH P15144, ROM 7906, AMNH FARB 221, FHSM VP 3, and KUVP 5033) identified KUVP 5033 as the most mature individual.

Most of the specimens recovered by this analysis as relatively immature (stages 1 through 8) are *T. proriger* and are individuals that were also recovered as juveniles and subadults (i.e., in the lower half of the ontogram) in the individual analysis (Fig. 6). All but one *T. kansasensis* are recovered at growth stages 8 and 9, and all specimens referred to *T. nepaeolicus* are recovered at stage 10. Finally, the most mature individuals (stages 11 through 13) are all large (i.e., TSL greater than 1000 mm and QH greater than 150 mm) *T. proriger* that were recovered as adults (i.e., in the upper half of the ontogram) in the individual analysis (Fig. 6). The following 13 growth stages are recovered:

Stage 1. This stage is not unambiguously defined by any character states (exemplar: *Tylosaurus* sp. neonate FHSM VP 14845).

Stage 2. The second stage is diagnosed by a quadrate tympanic ala that is thick (exemplar: *T. kansasensis* FHSM VP 9350).

Stage 3. The QH is between 50 – 99 mm, the quadrate infrastapedial process is present, the quadrate ala rim is defined, and the quadrate mandibular condyle is completely ossified (exemplars: *T. proriger* FMNH UR902 and *T. proriger* AMNH FARB 1592).

Stage 4. The quadrate suprastapedial process that is intermediate in length (exemplars: *T. nepaeolicus* holotype AMNH FARB 1565 and *T. proriger* RMM 5610).

Stage 5. The quadrate mandibular condyle is rounded (exemplars: *T. proriger* KUVP 66129).

Stage 6. The premaxillary rostrum is greater than or equal to 5% TSL, the quadrate infrastapedial process is rounded, QH is greater than or equal to 13% TSL, the parietal nuchal fossa is present, and the distance between the first and sixth dentary teeth is less than or equal to 23% TSL (exemplar: *T. proriger* AMNH FARB 4909).

Stage 7. The foramina on the premaxillary rostrum are small, the frontal-parietal suture flanges are small, the jugal posteroventral process is present, and the dentary length is between 60 and 56% lower jaw length (exemplar: *T. proriger* KUVP 1033).

Stage 8. The parietal posterior pegs are present and small and the pterygoid ectopterygoid process is thick (exemplars: *T. proriger* KUVP 28705, *T. kansasensis* FGM V 43, *T. kansasensis* holotype FHSM VP 2295, *T. kansasensis* FHSM VP 15632, and *T. kansasensis* FHSM VP 78). At this stage, all four *T. kansasensis* share a reversal to a premaxillary rostrum that is less than 5% TSL and FHSM VP 2295, FHSM VP 15632, and FHSM VP 78 share a reversal to a quadrate infrastapedial process that is absent.

Stage 9. This stage is diagnosed by a reversal to frontal-parietal suture flanges that are large and a dentary length that is less than or equal to 55% lower jaw length (exemplars: *T. kansasensis* FHSM VP 15631 and *T. kansasensis* FHSM VP 2495).

Stage 10. The premaxillary rostrum is distinctly knobbed, the frontal posterolateral processes are thick, there is a reversal to parietal posterior pegs that are absent, and the coronoid anterolateral notch is present and shallow (exemplars: *T. nepaeolicus* YPM 3974, *T. nepaeolicus* AMNH FARB 124/134, *T. nepaeolicus* FHSM VP 2209, *T. nepaeolicus* FHSM VP 7262, and *T. kansasensis* FMNH PR2103). At this stage, the exemplar specimens share a quadrate infrastapedial process that is subtle and pointed, parietal lateral borders that are convex, and 14 dentary teeth.

Stage 11. The TSL is between 1000 – 1499 mm and the QH is between 150 – 199 mm (exemplars: *T. proriger* KUVP 1032, *T. proriger* KUVP 50090, *T. proriger* USNM 8898, *T. proriger* FFHM 1997-10, *T. proriger* FMNH P15144*, T. proriger* ROM 7906*,* and *T. proriger* AMNH FARB 221). At this stage, the exemplar specimens share a premaxilla-maxilla suture that is m-shaped, and the relatively mature individuals (as recovered by the individual analysis (Fig. 6); FMNH P15144, ROM 7906, and AMNH FARB 221) share a reversal to a slender dentary.

Stage 12. The quadrate alar concavity is deep and the coronoid posteroventral process is present and fan-like (exemplar: *T. proriger* FHSM VP 3).

Stage 13. This stage is diagnosed by a TSL that is greater than or equal to 1500 mm and a QH that is greater than or equal to 200 mm (exemplar: *T. proriger* KUVP 5033).

Growth Series of *Te. nopcsai*

An exhaustive search recovered one ontogram with a length of 13 steps, a CI of 1.00, an HI of 0.00, an RI of 1.00, and an RC of 1.00 (Fig. 9). Under a Bremer decay test, resolution was lost

after the addition of one step. A total of three growth stages were identified; the analysis with an artificial adult did not recover a single most mature specimen, but a comparison of the total number of growth changes from the root of the ontogram recovered MNHN GOU 2 as the most mature individual. Character states that were unambiguously optimized as individual variation are listed in Table S2. The following growth stages are recovered:

Stage 1. This stage is not unambiguously defined by any character states (exemplars: MNHN GOU 4 and MNHN GOU 5). At this stage, the exemplar specimens share 14 or less pterygoid teeth.

Stage 2. The second stage is diagnosed by the presence of the quadrate infrastapedial process, a quadrate stapedial pit that is defined, and a quadrate mandibular condyle that is completely ossified (the holotype MNHN GOU 1).

Stage 3. This stage is diagnosed by the presence of an anteroventral corner on the quadrate ala (exemplar: MNHN GOU 2).

Growth Series of *M. hoffmannii*

An exhaustive search recovered one ontogram with a length of 42 steps, a CI of 0.93, an HI of 0.07, an RI of 0.73, and an RC of 0.68 (Fig. 10). Bremer decay analysis lost resolution after the addition of one step. A total of seven growth stages were identified; the analysis with an artificial adult did not recover a single most mature specimen, but comparison of the number of growth changes from the root of the ontogram recovered PRM 2546/CCMGE 10/2469 as the most mature individual. Character states that were unambiguously optimized as individual variation are listed in Table S2. The following growth stages are recovered:

Stage 1. This stage is not unambiguously defined by any character states (exemplars: IRSNB R 26).

Stage 2. The distance between the first and sixth dentary teeth is less than or equal to 25% TSL, the distance between the first and sixth dentary teeth is less than or equal to 35% dentary length, and the dentary bears 13 teeth (exemplar: TMM 313-1).

Stage 3. This stage is diagnosed by the presence of an anteroventral corner on the quadratic ala (exemplar: IRSNB R 27).

Stage 4. The QH is between 150 and 199 mm, the quadrate infrastapedial process is broad and pointed, and the dentary is deep (exemplars: NHMM 006696, ALMNH PV 1988.0018, and NJSM 11053). At this stage, the exemplar specimens share a QH that is greater than or equal to 13% TSL.

Stage 5. The ectopterygoid process of the pterygoid is thick (exemplar: TLAM NH.HR.2009.032.0001).

Stage 6. There is a reversal to a slender dentary (exemplar: *M. hoffmannii* holotype MNHN AC 9648).

Stage 7. This stage is diagnosed by a TSL greater than or equal to 1500 mm and a dentary length that is less than or equal to 65% lower jaw length (exemplar: PRM 2546/CCMGE 10/2469).

Congruence Between Size and Maturity

Scatterplots of size rank (TSL and QH) and growth rank data (Tables 4, 5, 6, 7, 8) that were used in the Spearman rank-order correlation tests are shown in Figures 11 through 15. A Shapiro-Wilk test was used to determine if there was sampling bias (i.e., skewed left or right) and revealed that all the growth rank data, size rank data, and measurement data, except for QH growth rank data for *T. nepaeolicus*, are normally distributed (Figs. 11, 12, 13, 14, 15). The Spearman rank-order test found a significant correlation between growth stage and both measures of size in *T. proriger* and *T. nepaeolicus*, both in the individual analyses and the analysis used to test for anagenesis (Figs. 11, 12, 13). Although a significant correlation between both measures of size and growth stage was also found for *Te. nopcsai* (Fig. 14), only two specimens could be included, and thus these results are tentative. The test did not find a significant correlation between TSL or QH and growth stage in *M. hoffmannii* (Fig. 15). All correlations between size and maturity are positive. Therefore, both TSL and QH and maturity usually covary in mosasaurs.

Discussion

Growth Series of *T. proriger*

The growth series of *T. proriger* has two bifurcations, at stages nine and 14 (Fig. 6). Following the reasoning of Frederickson and Tumarkin-Deratzian (2014), if either of these bifurcations represent sexual dimorphism, each sex should (1) independently develop a shared sequence of growth changes, since they are the same taxon, in addition to (2) developing unique morphological features that are hypothetically used for sexual display. The bifurcation at stage 14, in which three specimens share a distance between the first and sixth maxillary teeth that is greater than or equal to 25% TSL and a reversal to a QH between 100 – 149 mm, does not meet either of these criteria. The group of specimens at stage nine share a distance between the first and sixth dentary teeth that is less than or equal to 23% TSL and less than or equal to 35% dentary length, which develop independently at stages 13 and 15, respectively; however, none of the growth characters separating the specimens at stage nine from those at stages ten through 17 are obviously correlated with any kind of sexual display (e.g., thickening of the quadrate

suprastapedial and frontal posterolateral processes, presence of dentary predental dorsal ridge and knobbed premaxillary rostrum). If, however, these characters are correlated with being larger, it is possible that *T. proriger* was sexually dimorphic with respect to size – the TSL of the specimens at stage nine range from 610 mm to 813 mm (average: 712 mm), whereas the TSL of specimens from stage ten to stage 17 are generally larger, ranging from 585 mm to 1300 mm (average: 1032 mm). This hypothesis of size-based sexual dimorphism in *T. proriger*, as well as other mosasaurs, must be tested with the addition of more characters known to be dimorphic in extant squamates, such as growth rate (Frynta et al., 2010) and number of presacral vertebrae (Aplin, Fitch, and King, 2006).

The major growth changes of *T. proriger* are: development of processes on the premaxilla, frontal, jugal, pterygoid, quadrate, coronoid, and dentary; decrease in premaxillary foramina size; change in shape of the premaxilla-maxilla suture; ossification of the quadrate and basioccipital; enlargement of teeth relative to skull size; and a progressive deepening and enlargement of the skull (Fig. 6). The identification of RMM 5610 as a young individual in previous work is supported, but the identification (e.g., Jiménez-Huidobro, Simões, and Caldwell, 2016; Stewart and Mallon, 2018; Jiménez-Huidobro and Caldwell, 2019) of AMNH FARB 4909 as an adult is not (Fig. 6). The hypothesis of growth in *T. proriger* proposed here can be tested by adding more characters, particularly from the postcranial skeleton given there is evidence for ontogenetic variability in both axial and appendicular structures (Caldwell, 1996; Bell, 1997; Carpenter, 2017).

The Spearman rank-order test revealed a significant correlation between size rank and growth stage rank for both TSL ($r_{S(0.05,\ 18)} = 0.824$ $p < 0.001$) and QH ($r_{S(0.05,\ 17)} = 0.897$, $p < 0.001$), suggesting that both measures are reliable proxies for maturity in *T. proriger* (Fig. 11). This result is unexpected, given the oversampling of adults and subadults: apart from the *Tylosaurus* sp. neonate (FHSM VP 14845), this analysis only includes large (TSL greater than 500 mm) individuals. The correlation between size and maturity can be tested with the addition of significantly smaller, presumably juvenile, specimens.

Growth Series of *T. kansasensis* and *T. nepaeolicus*

The ontogram does not bifurcate and so it does not show evidence for sexual dimorphism, whereas the synonymy of *T. kansasensis* with *T. nepaeolicus* is supported (Figs. 4, 5); therefore, both taxa will be referred to as *T. nepaeolicus* henceforth. The major growth trends in *T. nepaeolicus* include: enlargement of processes on the premaxilla, frontal, quadrate, coronoid, and dentary; change in shape of the quadrate, parietal, and occipital condyle; changes in size of the premaxillary foramina; change in shape of the premaxilla-maxilla suture; ossification of the quadrate; enlargement of teeth relative to skull size; and an increase in the number of dentary teeth (Fig. 7). Like *T. proriger*, the growth series proposed here can be tested and expanded by adding more characters, particularly from the postcranial skeleton (Caldwell, 1996; Bell, 1997; Carpenter, 2017).

The Spearman rank-order test revealed a significant correlation between size rank and growth stage rank for TSL ($r_{S(0.05, 8)} = 0.874$, $p = 0.05$) and QH ($r_{S(0.05, 15)} = 0.719$ $p = 0.03$), suggesting that both are reliable proxies for maturity in this taxon (Fig. 12). Unlike *T. proriger*, multiple specimens in this dataset are rather small (TSL less than 500 mm, QH less than 50 mm), indicating a better representation of juveniles, in contrast to the large taxa (*T. proriger* and *M. hoffmannii*).

Validity of *T. kansasensis*. The ontogram does not bifurcate and therefore supports the synonymy of *T. kansasensis* with *T. nepaeolicus* (Figs. 5 and 7; Jiménez-Huidobro, Simões, and Caldwell, 2016). It does not unambiguously support previous hypotheses of growth patterns in the taxon given that *T. nepaeolicus* specimens are interspersed among those of *T. kansasensis* at the terminus of the ontogram; furthermore, although the holotype of *T. nepaeolicus* (stage 9) is recovered as more mature than the holotype of *T. kansasensis* (stage 8), there is no unambiguous support for this separation (Fig. 7). Most significantly, many of the diagnostic characters for *T. kansasensis* (Everhart, 2005) that could be identified (premaxilla foramina size, quadrate infrastapedial process, frontal midline crest, jugal posteroventral angle, quadrate ala thickness, quadrate alar concavity depth) were found to be juvenile characters and were also present in both *T. nepaeolicus* and *T. proriger*. First-hand observation and addition of specimens assigned to *T. nepaeolicus* is necessary to test this hypothesis, given that the current growth series includes nearly twice as many *T. kansasensis* as *T. nepaeolicus*.

Evidence for paedomorphy in *T. proriger*. Paedomorphy is the truncation of development in a descendent taxon relative to an ancestral taxon (Reilly, Wiley, and Meinhardt, 1997); therefore, the results of this project do not support the hypothesis that presence of the frontal dorsal midline crest in *T. proriger* is paedomorphic relative to *T. nepaeolicus* (Jiménez-Huidobro, Simões, and Caldwell, 2016). Absence of the crest in *T. nepaeolicus* is peramorphic – that is, an extension of development in a descendant taxon relative to an ancestral taxon (Reilly, Wiley, and Meinhardt, 1997) – relative to other mosasaurs, including *T. proriger*, because it is present in all specimens of *Te. nopcsai* (a basal russelosaurine; see Fig. 1) and *M. hoffmannii* (a derived mosasaurine; see Fig. 1) regardless of growth stage.

Although absence of the crest was not unambiguously optimized on the ontogram of *T. nepaeolicus*, the two specimens in which the crest is absent (AMNH FARB 124/134 and YPM 3974; Data S2) are recovered as relatively mature individuals (stage 11; Fig. 7). Because of the low number (seven) of *T. nepaeolicus* included in the ontogram, more data are necessary to test this hypothesis, given the crest is only absent in two *T. nepaeolicus* specimens out of the 35 that were coded. If the addition of more characters and specimens of *T. nepaeolicus* recovers absence of the crest as a mature character, then the addition of basal mosasaurs, such as the mosasauroid *Aigialosaurus* (Fig. 1), as well as other derived taxa (e.g. *Platecarpus*, *Prognathodon*) can help to trace the evolution of frontal crest development across the clade and for a more rigorous test of the hypothesis of paedomorphy of this character in *T. proriger*.

Anagenesis in *T. nepaeolicus* and *T. proriger*

The ontogram recovered by the analysis of all three *Tylosaurus* taxa supports the hypothesis of anagenesis in the clade (Fig. 8). The least mature individuals in the ontogram are nearly all juvenile and subadult *T. proriger*, the specimens of intermediate maturity are subadult and adult *T. nepaeolicus*, and the most mature individuals are large adult *T. proriger*. Furthermore, the placement of all *T. kansasensis* as less mature than *T. nepaeolicus* and among juvenile *T. proriger* is consistent with the hypothesis that *T. kansasensis* are juvenile *T. nepaeolicus*.

Several growth changes recovered in this analysis were also recovered in the individual analyses: thickening of the quadrate ala, quadrate mandibular condyle ossifies and becomes rounded, QH increases relative to TSL, premaxilla rostrum foramina size changes, frontal posterolateral processes thicken, and the knobbed premaxillary rostrum after which the genus is named grows in.

Anagenesis in WIS *Tylosaurus* was driven by peramorphosis (acceleration and extension of growth) in the following characters: skull size (TSL) and depth (QH) (Fig. 13), premaxillary rostrum length (greater than 5% TSL does not occur until relatively late in ontogeny in *T. nepaeolicus*, whereas it is present in subadult *T. proriger*), overall quadrate shape (Fig. 16; the quadrates of the most mature *T. nepaeolicus*, e.g. AMNH FARB 124/134, are morphologically most similar to juvenile *T. proriger*, e.g. FMNH UR902), quadrate suprastapedial process thickness, and coronoid posteroventral process shape (from single bump to fan-like). The hypothesis of anagenesis in North American *Tylosaurus* can be further tested by recovering growth series for *T. saskatchewanensis* and *T. pembinensis*, which lived after *T. proriger* during the late Campanian (Jiménez-Huidobro and Caldwell, 2019).

Revised diagnoses of *T. nepaeolicus* and *T. proriger*. Based on the growth patterns uncovered by this work (Figs. 6, 7, 8, 16), the following revisions to the diagnoses of *T. nepaeolicus* by Jiménez-Huidobro and Caldwell (2019) are made: (1) frontal dorsal midline crest generally present except in some relatively mature individuals; (2) lateral borders of parietal table slightly convex in adults; (3) the overall shape of the quadrate is semicircular and hook-like in juveniles and subadults, and relatively more dorsoventrally elongate in adults; (4) quadrate infrastapedial process absent in juveniles and poorly developed in adults; (5) 12 to 13 maxillary teeth; (6) ten to 15 dentary teeth; and (7) eight to ten pterygoid teeth in adults, possibly 11 or more in juveniles.

Based on the growth patterns uncovered by this work (Figs. 6, 7, 8, 16), the following revisions to the diagnoses of *T. proriger* by Jiménez-Huidobro and Caldwell (2019) are made: (1) the overall shape of the quadrate is columnar and distinctly taller than wide throughout growth; (2) quadrate infrastapedial process is well-developed and is subtle and pointed in juveniles and distinct, broad, and semicircular in adults; (3) quadrate tympanic ala is thin, wide, and flat throughout growth and the alar concavity is deep in adults; (4) 13 maxillary teeth; (5) 13 dentary teeth; and (6) ten pterygoid teeth.

Growth Series of *Te. nopcsai*

As in both species of *Tylosaurus*, the major growth changes in *Te. nopcsai* involve the ossification and development of the quadrate (Fig. 9). More specimens and characters are needed to identify other growth patterns in *Te. nopcsai*.

The Spearman rank-order test revealed a significant correlation between size rank and growth stage rank for both TSL ($r_{S(0.05, 2)} = 1.000$ $p < 0.001$) and QH ($r_{S(0.05, 2)} = 1.000$, $p < 0.001$), suggesting that both measures are reliable proxies for maturity in *Te. nopcsai* (Fig. 14). However, only two specimens had size data available for the test, and therefore the results must be tested further once additional specimens are discovered.

Growth Series of *M. hoffmannii*

The growth series of *M. hoffmannii* bifurcates at stage four, but it does not meet the criteria for sexual dimorphism outlined by Frederickson and Tumarkin-Deratzian (2014). The growth changes recovered in *M. hoffmannii* include: increase in TSL and QH; growth of quadrate processes; and deepening of the dentary (Fig. 10). More data from first-hand observation are needed to identify additional growth changes and resolve the polytomy of immature individuals.

The Spearman rank-order did not recover a significant correlation between size rank and growth stage rank for TSL ($r_{S(0.05, 6)} = 0.603$ $p = 0.205$) or QH ($r_{S(0.05, 7)} = 0.187$, $p = 0.688$), suggesting that neither TSL nor QH is a reliable proxy for maturity in *M. hoffmannii* (Fig. 15). This result was expected because of the small sample size and because of the large size of the specimens included – the smallest TSL in this project (IRSNB R 12) is 880 mm and the smallest QH (IRSNB R 26) is 125 mm (Table 1). Therefore, more specimens, especially true juveniles, are necessary to adequately test the congruence between size and maturity and clarify the pattern of *M. hoffmannii* TSL and QH throughout growth.

Sexual Dimorphism

The growth series did not recover evidence of skeletal sexual dimorphism in any of the four mosasaur taxa. This does not necessarily mean that mosasaurs were not sexually dimorphic, only that the characters in this analysis are not dimorphic. The hypothesis that the premaxillary predental rostrum is an ontogenetic, but not sexual, characteristic in *Tylosaurus* (Konishi, Jiménez-Huidobro, and Caldwell, 2018) is supported. These results are consistent with the absence of evidence for sexual dimorphism in any mosasaur, which itself is somewhat surprising given the frequency of sexual dimorphism in extant squamates (Schwarzkopf, 2005; Aplin, Fitch, and King, 2006; Openshaw and Keogh, 2014), including ocean-going species such as sea snakes and marine iguanas (Wikelski and Trillmich, 1997; Shine et al., 2002); excluding size, examples of sexually dimorphic characters in extant squamates include head width, trunk length (i.e., number of presacral vertebrae), and limb length (Schwarzkopf, 2005). The absence of morphological sexual dimorphism in mosasaurs will be tested further with the addition of more

growth characters – especially from the postcranial skeleton – as well as more specimens and taxa.

It is also possible that sexual dimorphism in mosasaurs could be present in histological data. In 2010, Frynta et al. found that adult male monitor lizards (*Varanus indicus*) are larger than females because the period of rapid growth is extended; if this is also the case in mosasaurs, these differences in growth rates are seen in histological analyses of limb bones (Houssaye and Tafforeau, 2012; Green, 2018). Another instance of sexual dimorphism in extant monitor lizards is bone density: in males, density tends to increase over time, whereas in females it decreases (de Buffrénil and Francillon-Vieillot, 2001). However, because this decrease in females is caused by skeletal calcium being used to produce eggshells (de Buffrénil and Francillon-Vieillot, 2001), this is unlikely to be seen in mosasaurs, which gave live birth (Caldwell and Lee, 2001; Field et al., 2015).

Cladistic Analysis of Growth as a Method to Test Taxon Validity

Besides traditional comparison of morphological characters, no thorough, objective tests of taxon validity using growth data have been attempted for any mosasaur taxon. By recovering growth changes and identifying instances of individual variation in multiple taxa, cladistic analysis of growth provides a robust test of taxon validity and the characters which purportedly diagnose them (see Figs. 4, 5). Taxon validity is a major problem in mosasaurs for multiple reasons, including insufficient descriptions and later loss or destruction of type specimens, paraphyly of genera, poor stratigraphic data, and past researchers' desire to name as many species as possible (Lively, 2019). This problem is only made worse by a lack of growth studies that include morphological data, which could be contributing to purported differences between taxa, and a general deficiency of recent hypothesis-driven work.

Mosasaurus is a particularly problematic group with respect to taxonomy and for which this approach could prove very useful in determining which species are valid and which are not. The results of this project do not conflict with the hypothesis of synonymy between *M. maximus* and *M. hoffmannii*; two specimens (TMM 313-1 and NJSM 11053) that were originally identified as *M. maximus* were included in the ontogram (Fig. 10), which does not bifurcate, and their positions (TMM 313-1 as one of the least mature individuals and NJSM 11053 as the most mature) do not support a taxon separate from *M. hoffmannii* (see Figs. 4, 5).

In addition to *M. maximus*, two other *Mosasaurus* taxa – *M. lemonnieri* and *M. conodon* – have been proposed to be synonymous with *M. hoffmannii* (Russell, 1967; Lingham-Soliar, 1995; Lingham-Soliar, 2000; Ikejiri and Lucas, 2015; Street and Caldwell, 2017); specimens of *M. lemonnieri* in particular have the potential to represent juveniles of *M. hoffmannii*, given the only major difference between them is that the skull of *M. lemonnieri* is generally smaller (around 500 mm – a size currently underrepresented in *M. hoffmannii*) and more slender than that of *M. hoffmannii* (Lingham-Soliar, 2000). By using a single cladistic analysis of growth including specimens of all *Mosasaurus* species for which synonymy has been proposed, as was done in this project for *T. kansasensis* and *T. nepaeolicus*, these hypotheses can be tested,

refining our understanding of mosasaur growth as well as their actual diversity in the Late Cretaceous.

Conserved Patterns of Growth in Mosasaurs

This project identified 17 growth characters shared by two or more taxa; these characters are: (1) increase in TSL (*T. proriger*, *M. hoffmannii*); (2) premaxilla rostrum becomes robust (*T. proriger*, *T. nepaeolicus*, *M. hoffmannii*); (3) change in premaxillary rostrum foramina size (*T. proriger*, *T. nepaeolicus*); (4) change in premaxilla-maxilla suture shape (*T. proriger*, *T. nepaeolicus*); (5) increase in QH (*T. proriger*, *T. nepaeolicus*, *M. hoffmannii*); (6) thickening of quadrate suprastapedial process (*T. proriger*, *T. nepaeolicus*); (7) change in quadrate infrastapedial process shape (*T. proriger*, *M. hoffmannii*); (8) increase in QH relative to TSL (*T. proriger*, *T. nepaeolicus*); (9) presence of an anteroventral corner of the quadrate tympanic ala (*Te. nopcsai*, *M. hoffmannii*); (10) ossification of the quadrate mandibular condyle (*T. proriger*, *T. nepaeolicus*, *Te. nopcsai*); (11) mandibular condyle of the quadrate becoming rounded (*T. proriger*, *T. nepaeolicus*); (12) thickening of frontal posterolateral processes (*T. proriger*, *T. nepaeolicus*); (13) deepening of the dentary (*T. proriger*, *M. hoffmannii*); (14) development of a dorsal ridge on the predentary process of the dentary (*T. proriger*, *T. nepaeolicus*); (15) change in the length of the dentary relative to lower jaw length (*T. proriger*, *M. hoffmannii*); (16) presence of an anterolateral notch on the coronoid (*T. nepaeolicus*, *M. hoffmannii*); and (17) growth of the coronoid posteroventral process (*T. proriger*, *T. nepaeolicus*). These shared growth characters are shown on a simplified cladogram in Figure 17.

These results reject previous hypotheses that variation of mosasaur quadrates is ontogenetically uninformative (Jiménez-Huidobro, Simões, and Caldwell, 2016; Stewart and Mallon, 2018), where all taxa show unambiguous changes to the shape of the quadrate and its processes throughout growth (Fig. 16). This suggests that the quadrate – particularly the thickness of the suprastapedial process, depth and thickness of the tympanic ala, and the presence and shape of the infrastapedial processes – should not be used to diagnose mosasaur taxa without an assessment of maturity. These results are not surprising, given that growth variation is seen in the quadrates of extant squamates (Paluh, Olgun, and Bauer, 2018). Because the shape of the quadrate in squamates is directly related to hearing ability and skull kinesis (LeBlanc, Caldwell, and Lindgren, 2013; Paluh, Olgun, and Bauer, 2018; Palci et al., 2019), future work is necessary to investigate the potential for niche partitioning between mosasaur growth stages.

Although size and maturity covary in every taxon, there is clearly an oversampling of adults where multiple individuals are recovered at the same growth stage. Therefore, more characters must be identified and coded to test these low-resolution results. This can be resolved though first-hand observation and measurements of specimens, especially *M. hoffmannii* and the other potentially synonymous *Mosasaurus* species. Also, several skulls in this project have associated vertebrae and limb bones; future work including histological data could be used to calibrate the growth series recovered here to chronological age and further test hypotheses of the relationship between size, maturity, and age and well as sexual dimorphism and ontogenetic

niche partitioning (Wiffen et al., 1995; de Buffrénil and Francillon-Vieillot, 2001; Frynta et al., 2010; Houssaye and Tafforeau, 2012; Green, 2018).

The size of the foramina on the premaxillary rostrum were recovered as ontogenetically informative in both species of *Tylosaurus* (Figs. 6, 7). Recent work on the tylosaurine *Taniwhasaurus antarcticus* has found internal branching structures, hypothesized to be part of the neurovascular system, associated with these foramina (Álvarez–Herrera, Agnolin, and Novas, 2020). Future work can investigate whether these internal structures are also present in other mosasaurs, including *Tylosaurus*, and whether they vary with growth as well.

No pattern of pterygoid tooth count was unambiguously recovered in these analyses, however, the number of pterygoid teeth could potentially be indicators of relative maturity in mosasaurs, given that their presence and number vary ontogenetically in extant lizards (Barahona and Barbadillo, 1998; Skawiński, Borczyk, and Turniak, 2017). Mosasaur pterygoid teeth have largely been ignored in the literature with respect to both ontogeny and phylogeny, and so future studies that include them are required to better understand their relevance to mosasaur development and evolution. For example, the basalmost taxon in this project, *Te. nopcsai*, has nearly double the number of pterygoid teeth than the other three taxa, and a relatively immature *T. nepaeolicus* specimen (FHSM VP 15632) has more pterygoid teeth (greater than 11) than more mature specimens (usually between eight and ten; Table 2).

Despite many studies that have investigated mosasaur phylogeny (Russell, 1967; Bell, 1997; Simões et al., 2017; Jiménez-Huidobro and Caldwell, 2019), the evolutionary relationships within Mosasauroidea remain unclear; the identification of shared growth characters can provide evidence to support or reject current hypotheses of relationships between mosasaurs and their extant relatives. In order to completely investigate ancestral patterns of growth in mosasaurs, growth series for basal mosasaurs, such as *Aigialosaurus*, as well as more derived taxa spanning a greater breadth of the phylogeny, such as *Clidastes*, *Platecarpus*, and *Prognathodon* (Fig. 1), must be recovered.

Conclusions

In conclusion: (1) a growth series was recovered for each taxon; (2) synonymy of *T. kansasensis* with *T. nepaeolicus* and the hypothesis that *T. kansasensis* represent juveniles of *T. nepaeolicus* is supported; (3) the hypothesis that *T. nepaeolicus* and *T. proriger* are a single anagenetic lineage is supported, where speciation was driven by peramorphy; (4) there is no evidence for skeletal sexual dimorphism in any taxon; (5) the absence of a frontal dorsal midline crest in *T. nepaeolicus* is peramorphic relative to other mosasaur taxa; and (6) 17 conserved patterns of growth were recovered across Mosasauridae.

With the addition of extant relatives (e.g., monitor lizards, iguanas, and snakes), ontogenetic data can be used to hypothesize phylogenetic position of Mosasauroidea and identify the heterochronic processes that shaped the land-sea transition of mosasaur ancestors. For example, in squamates, the overall shape of an animal's quadrate is related to what type of

habitat it occupies (e.g., terrestrial, aquatic, or fossorial) (Palci et al., 2019), and squamate quadrates change in shape throughout ontogeny (Fig. 16; Bhullar, 2012; Paluh, Olgun, and Bauer, 2018). Therefore, through the comparison of patterns of growth between extant terrestrial and semi-aquatic squamates to those seen across Mosasauroidea, the changes in quadrate shape that facilitate the transition from land to sea can be traced.

Once they are identified, ontogenetic changes that are unique to a taxon can help to recover evolutionary relationships (i.e., be used as phylogenetic characters) (Bhullar, 2012). One growth character recovered in this project – decrease of the posteroventral angle of the jugal in *T. nepaeolicus* throughout growth (Fig. 7) – was found by Bhullar (2012) to be apomorphic of Varanoidea. Despite the ambiguity with respect to the position of Mosasauroidea within Squamata (Russell, 1967; Carrol and DeBraga, 1992; Caldwell, Carroll, and Kaiser, 1995; Lee, 1997; Caldwell, 1999; Reeder et al., 2015; Simões et al., 2017), this character is almost certainly plesiomorphic in the common ancestor of Varanoidea and Mosasauroidea. The recovery of shared patterns of growth that unite mosasaurs with their extant relatives has the potential to resolve the phylogenetic relationships of Toxicofera (iguanas, anguimorph lizards, and snakes; Reeder et al., 2015) and provide a comparative point of reference for predicting the growth patterns of fossil taxa with low sample sizes (Witmer, 1995; Bhullar, 2012).

Finally, comparison of growth patterns with other secondarily aquatic taxa, both extant (e.g., sirenians, pinnipeds, cetaceans, turtles) and extinct (e.g., thalattosuchians, plesiosaurs, ichthyosaurs), is necessary to uncover the heterochronic processes that drive amniote land-sea transitions. For example, in 2020, Schwab et al. found that, in the evolution of thalattosuchians, a lineage of fully aquatic crocodylomorphs, the inner ear labyrinth became more thick and compact gradually; this is different from cetaceans, which evolved relatively small inner ear labyrinths very quickly, and suggests that the semiaquatic phase of thalattosuchian evolution lasted longer than that of cetaceans (Schwab et al., 2020). The advantage of comparing this and other features associated with an aquatic lifestyle (e.g., shortening of long bones, hyperphalangy, nostril retraction, increase in orbit size) across lineages and in an ontogenetic context is that it can identify the heterochronic processes that drove each transition and determine whether each instance is novel or convergent with respect to fundamental developmental mechanisms.

Institutional Abbreviations

AMNH, American Museum of Natural History, New York, New York; **CCMGE**, Chernyshev's Central Museum of Geological Exploration, Saint Petersburg, Russia; **CMN**, Canadian Museum of Nature, Aylmer, Quebec; **FFHM**, Fick Fossil and History Museum, Oakley, Kansas; **FHSM**, Fort Hays Sternberg Museum, Fort Hays, Kansas; **FGM**, Fryxell Geology Museum, Augustana College, Rock Island, Illinois; **FMNH**, Field Museum of Natural History, Chicago, Illinois; **HMG**, Hobetsu Museum, Hokkaido, Japan; **IRSNB**, Institut Royal des Sciences Naturelles de Belgique, Brussels, Belgium; **KUVP**, University of Kansas Museum of Natural History, Lawrence, Kansas; **LACMNH**, Los Angeles County Museum, Los Angeles, California; **MCZ**,

Museum of Comparative Zoology, Harvard University, Cambridge, Massachusetts; **MNHN**, Muséum National d'Histoire Naturelle, Paris, France; **NHMM**, Natuurhistorisch Museum Maastricht, Maastricht, the Netherlands; **NHMUK**, Natural History Museum, London, United Kingdom; **NJSM**, New Jersey State Museum, Trenton, New Jersey; **PRM**, Penza Regional Museum, Penza, Russia; **RMM**, Red Mountain Museum, Birmingham, Alabama; **TSMHN**, Teylers Museum, Spaarne, the Netherlands; **TLAM**, Timber Lake and Area Museum, Timber Lake, South Dakota; **TMM**, Texas Memorial Museum, University of Texas, Austin, Texas; **TMP**, Royal Tyrrell Museum of Paleontology, Drumheller, Alberta; **USNM**, United States National Museum, Washington, D. C.

Acknowledgements

I thank T. Carr for mentorship and feedback on this project, and T. Burling, T. Gamble, A. Griffing, and B. Holbach for general help, support, and advice. Additionally, I thank M. Everhart (FHSM) for having specimen photos and other resources available on his website and for clarifying information about AMNH FARB 221, FGM V 43, and KUVP 5033. I thank W. Simpson (FMNH) and A. Stroup (FMNH) for access to FMNH specimens, C. Mehling and M. Norell for access to AMNH specimens, S. Kornreich Wolf (FGM) for access to FGM V 43, C. Shelburne (FHSM) for access to FHSM specimens, and M. Sims (KU) and A. Whitaker (KU) for access to (and, for KUVP 5033, help maneuvering) KU specimens. The program TNT was made available by the Willi Hennig Society. I also thank Carthage College for funding travel to present preliminary results of this project at both the 79th Annual Meeting of the Society of Vertebrate Paleontology in Brisbane, QLD, and, with permission from J. Mathews, at the 22nd Annual PaleoFest at the Burpee Museum of Natural History in Rockford, IL. Finally, I thank J. Mallon (CMN) and T. Konishi (University of Cincinnati) for additional information about FFHM 1997-10 and CMN 8162, respectively, and P. Jiménez-Huidobro for clarifying some of the growth characters.

References

Álvarez–Herrera, G., F. Agnolin, and F. Novas. 2020. A rostral neurovascular system in the mosasaur *Taniwhasaurus antarcticus*. The Science of Nature 107:1-5.

Aplin, K. P., A. J. Fitch, and D. J. King. 2006. A new species of *Varanus merrem* (Squamata: Varanidae) from the Pilbara region of Western Australia, with observations on sexual dimorphism in closely related species. Zootaxa 1313(1313):1-38.

Barahona, F., and L. J. Barbadillo. 1998. Inter-and intraspecific variation in the post-natal skull of some lacertid lizards. Journal of Zoology 245:393-405.

Bardet, N., X. P. Suberbiola, and N. E. Jalil. 2003. A new mosasauroid (Squamata) from the Late Cretaceous (Turonian) of Morocco. Comptes Rendus Palevol 2:607-616.

Bell, G. L. 1997. A phylogenetic revision of North American and Adriatic Mosasauroidea; pp. 293-332 in J. M. Callaway and E. Nicholls (eds.), Ancient Marine Reptiles. Academic Press, Cambridge, Massachusetts.

Bhullar, B. A. S. 2012. A phylogenetic approach to ontogeny and heterochrony in the fossil record: cranial evolution and development in anguimorphan lizards (Reptilia: Squamata). Journal of Experimental Zoology Part B: Molecular and Developmental Evolution 318(7):521-530.

Brinkman, D. 1988. Size-independent criteria for estimating relative age in *Ophiacodon* and *Dimetrodon* (Reptilia, Pelycosauria) from the Admiral and lower Belle Plains formations of west-central Texas. Journal of Vertebrate Paleontology 8:172-180.

Brochu, C. A. 1996. Closure of neurocentral sutures during crocodilian ontogeny: implications for maturity assessment in fossil archosaurs. Journal of Vertebrate Paleontology 16:49-62.

Caldwell, M. W., R. L. Carroll, and H. Kaiser. 1995. The pectoral girdle and forelimb of *Carsosaurus marchesetti* (Aigialosauridae), with a preliminary phylogenetic analysis of mosasauroids and varanoids. Journal of Vertebrate Paleontology 15:516-531.

Caldwell, M. W. 1996. Ontogeny and phylogeny of the mesopodial skeleton in mosasauroid reptiles. Zoological Journal of the Linnean Society, 116: 407-436.

Caldwell, M. W. 1999. Squamate phylogeny and the relationships of snakes and mosasauroids. Zoological Journal of the Linnean Society 125:115-147.

Caldwell, M. W. 2007. Ontogeny, anatomy and attachment of the dentition in mosasaurs (Mosasauridae: Squamata). Zoological Journal of the Linnean Society, 149:687-700.

Caldwell, M. W., and M. S. Lee. 2001. Live birth in Cretaceous marine lizards (mosasauroids). Proceedings of the Royal Society of London. Series B: Biological Sciences, 268:2397-2401.

Carpenter, J. A. 2017. Locomotion and skeletal morphology of Late Cretaceous mosasaur, *Tylosaurus proriger*. University honors program thesis, Georgia Southern University, Statesboro, Georgia, 28 pp.

Carr, T. D. 1999. Craniofacial ontogeny in tyrannosauridae (Dinosauria, Coelurosauria). Journal of vertebrate Paleontology 19:497-520.

Carr, T. D., and T. E. Williamson. 2004. Diversity of late Maastrichtian Tyrannosauridae (Dinosauria: Theropoda) from western North America. Zoological Journal of the Linnean Society 142:479-523.

Carr, T. D., D. J. Varricchio, J. C. Sedlmayr, E. M. Roberts, and J. R. Moore. 2017. A new tyrannosaur with evidence for anagenesis and crocodile-like facial sensory system. Scientific reports 7:44942.

Carroll, R. L., and M. DeBraga. 1992. Aigialosaurs: mid-Cretaceous varanoid lizards. Journal of Vertebrate Paleontology, 12(1):66-86.

Cope, E. D. 1869. Remarks on *Macrosaurus proriger*. In Proceedings of the Academy of Natural Sciences of Philadelphia, 11, 123.

1071 Cope, E. D. 1874. Review of the Vertebrata of the Cretaceous period found west of the
1072 Mississippi River. Bulletin of the United States Geological and Geographical Survey of
1073 the Territories/Department of the Interior 1/2, pp. 3-48.
1074 Cuvier, G. 1808. Sur le grand animal fossile des carrières de Maestricht. Frères Levrault.
1075 de Buffrénil, V., and H. Francillon-Vieillot. 2001. Ontogenetic changes in bone compactness in
1076 male and female Nile monitors (*Varanus niloticus*). Journal of Zoology 254:539-546.
1077 Everhart, M. J. 2005. *Tylosaurus kansasensis*, a new species of tylosaurine (Squamata,
1078 Mosasauridae) from the Niobrara Chalk of western Kansas, USA. Netherlands Journal of
1079 Geosciences, 84:231-240.
1080 Everhart, M. J. 2017. Oceans of Kansas: a Natural History of the Western Interior Sea (second
1081 edition). Indiana University Press, Bloomington, Indiana, 490 pp.
1082 Field, D. J., A. LeBlanc, A. Gau, and A. D. Behlke. 2015. Pelagic neonatal fossils support
1083 viviparity and precocial life history of Cretaceous mosasaurs. Paleontology 58:401-407.
1084 Frederickson, J. A., and A. R. Tumarkin-Deratzian. 2014. Craniofacial ontogeny in *Centrosaurus*
1085 *apertus*. PeerJ, 2, e252.
1086 Frynta, D., P. Frýdlová, J. Hnízdo, O. Šimková, V. Cikánová, and P. Velenský. 2010. Ontogeny
1087 of sexual size dimorphism in monitor lizards: males grow for a longer period, but not at a
1088 faster rate. Zoological science 27:917-924.
1089 Goloboff, P. A., and S. A. Catalano. 2016. TNT version 1.5, including a full implementation of
1090 phylogenetic morphometrics. Cladistics 32:221-238.
1091 Green, C. C. 2018. Osteohistology and skeletochronology of an ontogenetic series of Clidastes
1092 (Squamata: Mosasauridae): growth and metabolism in basal mosasaurids. Master's thesis,
1093 Fort Hays State University, Hays, Kansas, 51 pp.
1094 Grigoriev, D. V. 2014. Giant *Mosasaurus hoffmanni* (Squamata, Mosasauridae) from the
1095 Late Cretaceous (Maastrichtian) of Penza, Russia. Proceedings of the Zoological
1096 Institute RAS 318:148-167.
1097 Harrell, T. L., and J. E. Martin. 2015. A mosasaur from the Maastrichtian Fox Hills
1098 Formation of the northern Western Interior Seaway of the United States and the
1099 synonymy of *Mosasaurus maximus* with *Mosasaurus hoffmanni* (Reptilia:
1100 Mosasauridae). Netherlands Journal of Geosciences 94:23-37.
1101 Horner, J. R., D. J. Varricchio, and M. B. Goodwin. 1992. Marine transgressions and the
1102 evolution of Cretaceous dinosaurs. Nature 358:59-61.
1103 Houssaye, A., and N. Bardet. 2013. A baby mosasauroid (Reptilia, Squamata) from the Turonian
1104 of Morocco–*Tethysaurus* ‘junior’ discovered? Cretaceous Research 46:208-215.
1105 Houssaye, A., and P. Tafforeau. 2012. What vertebral microanatomy reveals about the ecology
1106 of juvenile mosasaurs (Reptilia, Squamata). Journal of Vertebrate Paleontology 32:1042-
1107 1048.
1108 IBM Corp. 2019. IBM SPSS Statistics for Windows, Version 26.0. Armonk, NY: IBM Corp.
1109 Ikejiri, T., and S. G. Lucas. 2015. Osteology and taxonomy of *Mosasaurus conodon* Cope
1110 1881 from the Late Cretaceous of North America. Netherlands Journal of

Geosciences, 94:39-54.
Jiménez-Huidobro, P., T. R. Simões, and M. W. Caldwell. 2016. Re-characterization of *Tylosaurus nepaeolicus* (Cope, 1874) and *Tylosaurus kansasensis* Everhart, 2005: ontogeny or sympatry? Cretaceous Research 65:68-81.
Jiménez-Huidobro, P., and M. W. Caldwell. 2019. A new hypothesis of the phylogenetic relationships of the Tylosaurinae (SQUAMATA: MOSASAUROIDEA). Frontiers in Earth Science 7:47.
Konishi, T., P. Jiménez-Huidobro, and M. W. Caldwell. 2018. The smallest-known neonate individual of *Tylosaurus* (Mosasauridae, Tylosaurinae) sheds new light on the Tylosaurine rostrum and heterochrony. Journal of Vertebrate Paleontology 1-11.
LeBlanc, A. R., M. W. Caldwell, and J. Lindgren. 2013. Aquatic adaptation, cranial kinesis, and the skull of the mosasaurine mosasaur *Plotosaurus bennisoni*. Journal of Vertebrate Paleontology 33:349-362.
Lee, M. S. 1997. The phylogeny of varanoid lizards and the affinities of snakes. Philosophical Transactions of the Royal Society of London. Series B: Biological Sciences 352:53-91.
Leidy, J. 1873. Contributions to the extinct vertebrate fauna of the western territories (Vol. 1). US Government Printing Office.
Lingham-Soliar, T. 1995. Anatomy and functional morphology of the largest marine reptile known, *Mosasaurus hoffmanni* (Mosasauridae, Reptilia) from the Upper Cretaceous, Upper Maastrichtian of the Netherlands. Philosophical Transactions of the Royal Society of London. Series B: Biological Sciences 347:155-180.
Lingham-Soliar, T. 2000. The mosasaur *Mosasaurus lemonnieri* (Lepidosauromorpha, Squamata) from the Upper Cretaceous of Belgium and The Netherlands. Paleontological Journal, 34.
Lively, J. R. Taxonomy and historical inertia: *Clidastes* (Squamata: Mosasauridae) as a case study of problematic paleobiological taxonomy. Alcheringa: An Australasian Journal of Palaeontology 42:516-527.
Longrich, N. R., and D. J. Field. 2012. *Torosaurus* is not *Triceratops*: ontogeny in chasmosaurine ceratopsids as a case study in dinosaur taxonomy. PloS one 7:e32623.
Maddison, W.P. and D.R. Maddison. 2018. Mesquite: a modular system for evolutionary analysis. Version 3.51. http://www.mesquiteproject.org.
Mantell, G.A., 1829. A tabular arrangement of the organic remains of the county of Sussex. Geological Society of London Transactions, 2nd series 3: 201-216.
Mulder, E. W. 1999. Transatlantic latest Cretaceous mosasaurs (Reptilia, Lacertilia) from the Maastrichtian type area and New Jersey. Geologie en Mijnbouw 78:281-300.
Openshaw, G. H., and J. S. Keogh. 2014. Head shape evolution in monitor lizards (*Varanus*): interactions between extreme size disparity, phylogeny and ecology. Journal of Evolutionary Biology, 27:363-373.
Palci, A., M. W. Caldwell, M. N. Hutchinson, T. Konishi, and M. S. Lee. 2019. The morphological diversity of the quadrate bone in squamate reptiles as revealed by high-

resolution computed tomography and geometric morphometrics. Journal of anatomy.
Paluh, D. J., K. Olgun, and A. M. Bauer. 2018. Ontogeny, but not sexual dimorphism, drives the intraspecific variation of quadrate morphology in *Hemidactylus turcicus* (Squamata: Gekkonidae). Herpetologica 74:22-28.
Pellegrini, R. 2007. Skeletochronology of the limb elements of mosasaurs (Squamata; Mosasauridae). Transactions of the Kansas Academy of Science 110:83-100.
Reeder, T. W., T. M. Townsend, D. G. Mulcahy, B. P. Noonan, P. L. Wood Jr., J. W. Sites Jr., and J. J. Wiens. 2015. Integrated analyses resolve conflicts over squamate reptile phylogeny and reveal unexpected placements for fossil taxa. PLoS one 10:e0118199.
Reilly, S. M., E. O. Wiley, and D. J. Meinhardt. 1997. An integrative approach to heterochrony: the distinction between interspecific and intraspecific phenomena. Biological Journal of the Linnean Society 60:119-143.
Rozhdestvensky, A. K. 1965. Growth changes in Asian dinosaurs and some problems of their taxonomy. Paleontologicheskii Zhurnal 1965:95-100.
Russell, D. A. 1967. Systematics and morphology of American mosasaurs. Yale University Peabody Museum of Natural History Bulletin 23:1-241.
Scannella, J. B., D. W. Fowler, M. B. Goodwin, and J. R. Horner. 2014. Evolutionary trends in *Triceratops* from the Hell Creek formation, Montana. Proceedings of the National Academy of Sciences 111:10245-10250.
Schwab, J. A, M. T. Young, J. M. Neenan, S. A. Walsh, L. M. Witmer, Y. Herrera, R. Allain, C. A. Brochu, J. N. Choiniere, J. M. Clark, K. N. Dollman, S. Etchesk, G. Fritsch, P. M. Gignac, A. Ruebenstahl, S. Sachs, A. H. Turner, P. Vignaud, E. W. Wilberg, X. Xu, L. E. Zanno, and S. L. Brusatte. 2020. Inner ear sensory system changes as extinct crocodylomorphs transitioned from land to water. Proceedings of the National Academy of Sciences 117:10422-10428.
Schwarzkopf, L. 2005. Sexual dimorphism in body shape without sexual dimorphism in body size in water skinks (*Eulamprus quoyii*). Herpetologica 61:116-123.
Shine, R., R. Reed, S. Shetty, and H. Cogger. 2002. Relationships between sexual dimorphism and niche partitioning within a clade of sea-snakes (*Laticaudinae*). Oecologia 133:45-53.
Simões, T. R., O. Vernygora, I. Paparella, P. Jimenez-Huidobro, and M. W. Caldwell. 2017. Mosasauroid phylogeny under multiple phylogenetic methods provides new insights on the evolution of aquatic adaptations in the group. PloS one 12:e0176773.
Skawiński, T., B. Borczyk, and E. Turniak. 2017. Variability of pterygoid teeth in three species of *Podarcis* lizards and the utility of palatal dentition in lizard systematics. Belgian Journal of Zoology 147(2).
Stewart, R. F., and J. Mallon. 2018. Allometric growth in the skull of *Tylosaurus proriger* (Squamata: Mosasauridae) and its taxonomic implications. Vertebrate Anatomy Morphology Paleontology 6:75.
Street, H. P., and M. W. Caldwell. 2017. Rediagnosis and redescription of *Mosasaurus hoffmannii* (Squamata: Mosasauridae) and an assessment of species assigned to the genus *Mosasaurus*. Geological Magazine 154:521-557.

1192 Swofford, D. A. 2003. PAUP* 4.0. Sinauer Associates, Sunderland, Massachusetts.
1193 Wiffen, J., V. De Buffrénil, A. De Ricqlès, and J. M. Mazin. 1995. Ontogenetic evolution of
1194 bone structure in Late Cretaceous Plesiosauria from New Zealand. Geobios 28:625-640.
1195 Wikelski, M., and F. Trillmich. 1997. Body size and sexual size dimorphism in marine iguanas
1196 fluctuate as a result of opposing natural and sexual selection: an island comparison.
1197 Evolution 51:922-936.
1198 Wilson, J. P., M. J. Ryan, and D. C. Evans. 2020. A new, transitional centrosaurine ceratopsid
1199 from the Upper Cretaceous Two Medicine Formation of Montana and the evolution of
1200 the '*Styracosaurus*-line' dinosaurs. Royal Society Open Science 7:200284.
1201 Witmer, L. M. 1995. The extant phylogenetic bracket and the importance of reconstructing soft
1202 tissues in fossils. Functional morphology in vertebrate paleontology 1:19-33.

Figure 1

Simplified phylogeny of major mosasaur taxa based on the cladistic analyses of Jiménez-Huidobro and Caldwell (2019) and Simões et al. (2017).

Asterisks indicate taxa included in this project.

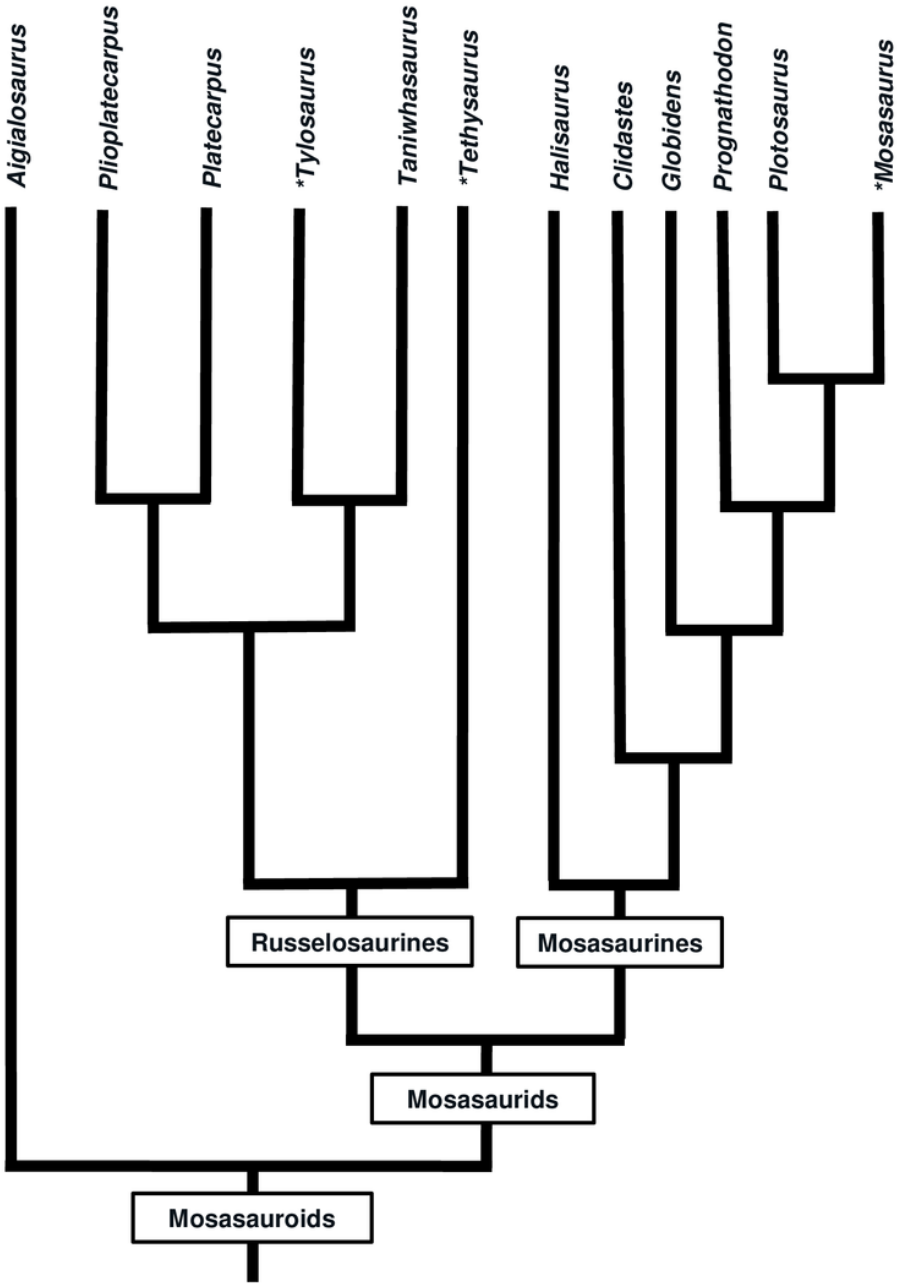
Aigialosaurus
Plioplatecarpus
Platecarpus
*Tylosaurus
Taniwhasaurus
*Tethysaurus
Halisaurus
Clidastes
Globidens
Prognathodon
Plotosaurus
*Mosasaurus
Russelosaurines
Mosasaurines
Mosasaurids
Mosasauroids

Figure 2

Comparison between hypothetical low-resolution and high-resolution growth series.

(A) In a low-resolution growth series, multiple individuals are grouped into vague sets. (B) In a high-resolution growth series, each growth stage only has a single individual.

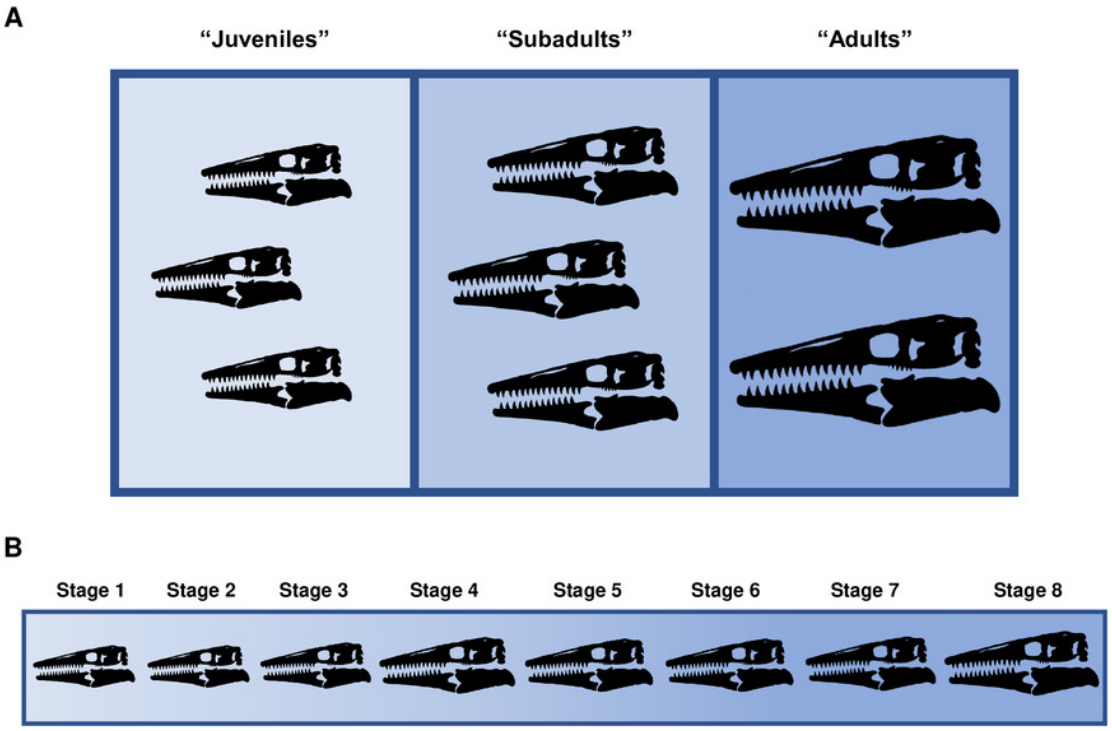

Figure 3

Possible scenarios when determining the most mature individual.

In each scenario, a cladistic analysis has recovered hypothetical specimens “Y” (light gray) and “Z” (black) at the terminus of the ontogram. The most mature individual(s) is indicated by an arrowhead. (A) The analysis with an artificial adult is successful; the artificial adult is recovered closest to specimen “Y,” indicating that it is the most mature. (B) The analysis with the artificial adult fails to recover a single most mature specimen; the artificial adult is not closer to specimen “Y” or specimen “Z.” (C) Should the analysis with the artificial adult fail, the specimen with the most accumulated growth changes (synontomorphies) is considered the most mature; in this scenario, the most mature individual is specimen “Y,” with a total of four synontomorphies.

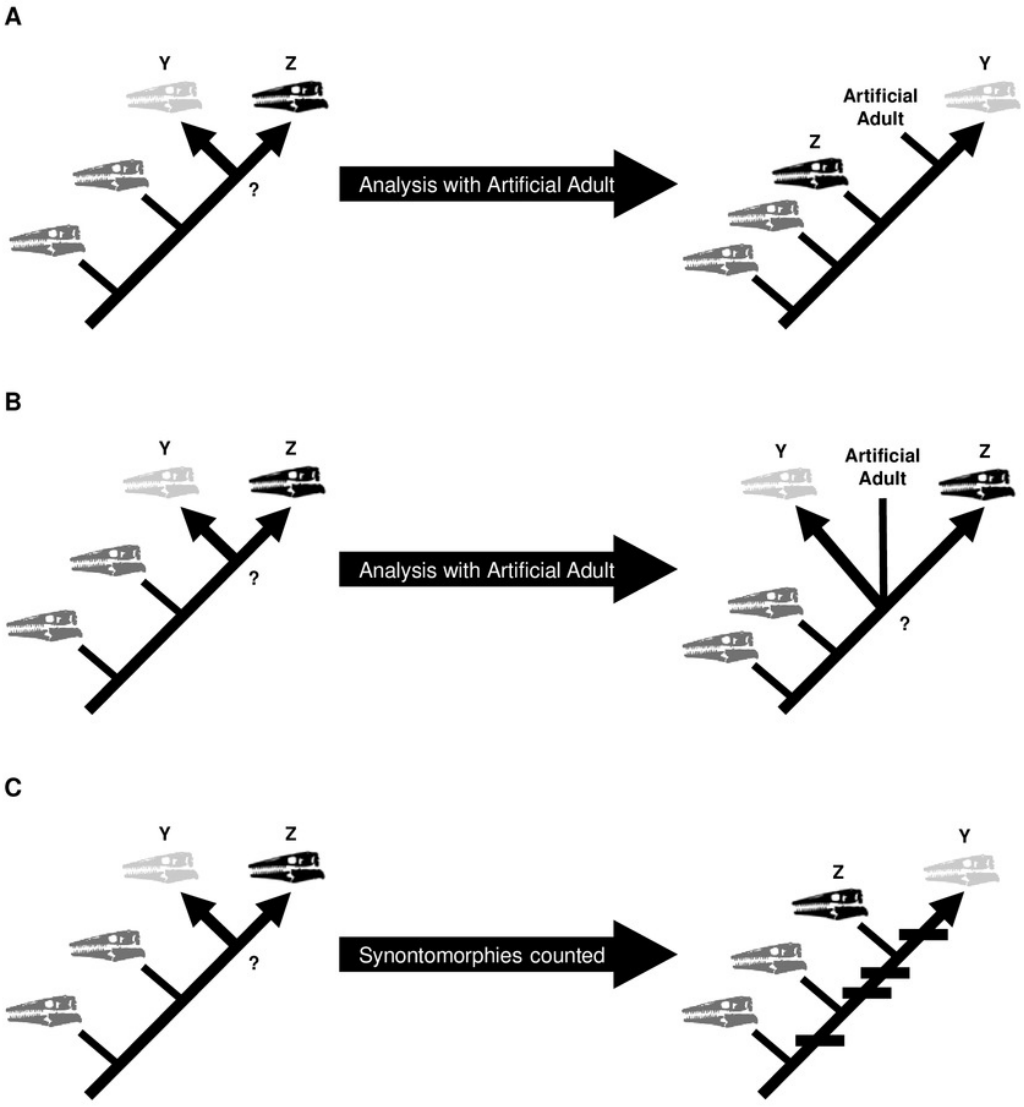
A
Y
Z
?
Analysis with Artificial Adult
Y
Artificial Adult
Z
B
Y
Z
?
Analysis with Artificial Adult
Y
Artificial Adult
Z
?
C
Y
Z
?
Synontomorphies counted
Y
Z

Figure 4

Summary of potential outcomes for the growth series recovered by the cladistic analysis.

(A) The specimens included in the analysis represent a single taxon without sexual dimorphism. (B) The specimens in the analysis represent either a single taxon that is sexually dimorphic or two separate taxa with morphologically similar juveniles. (C) The specimens in the analysis represent either a single taxon that is sexually dimorphic with an oversampling of adults or two separate taxa. (D) The analysis recovers two or more groups of specimens defined by shared instances of individual variation; these groups could represent different taxa or sexual dimorphism.

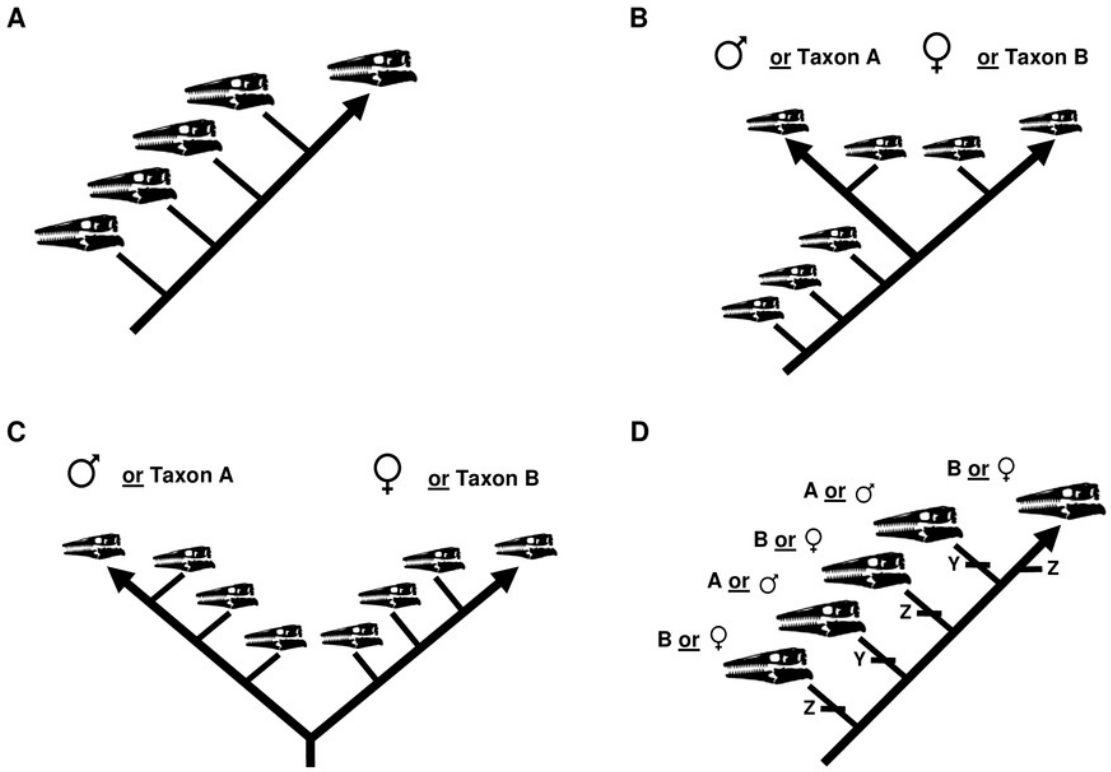
A
B
♂ or Taxon A
♀ or Taxon B
C
♂ or Taxon A
♀ or Taxon B
D
A or ♂
B or ♀
B or ♀
A or ♂
B or ♀
Y
Z
Z
Y
Z

Figure 5

Summary of potential outcomes for the analysis of the data matrix including *T. kansasensis* and *T. nepaeolicus*.

Hypothetical *T. nepaeolicus* specimens are represented by black skulls and hypothetical *T. kansasensis* specimens are represented by gray skulls. (A) If the current hypothesis is supported and *T. kansasensis* represent juveniles of *T. nepaeolicus* (Jiménez-Huidobro, Simões, and Caldwell, 2016), most or all *T. kansasensis* specimens will be recovered as less mature than most or all *T. nepaeolicus* specimens. (B) If *T. kansasensis* represent juveniles of *T. nepaeolicus*, and the taxon is sexually dimorphic, most or all *T. kansasensis* specimens will be recovered as less mature than most or all *T. nepaeolicus* specimens and before the onset of sexual maturity (represented by a bifurcation in the ontogram). (C) If *T. kansasensis* and *T. nepaeolicus* represent the same taxon but neither is necessarily all adults or all juveniles, and sexual dimorphism is absent, the specimens will be interspersed with each other on the tree. (D) If *T. kansasensis* and *T. nepaeolicus* represent the same taxon but neither is necessarily all adults or all juveniles, and sexual dimorphism is present, the specimens will be interspersed with each other on the tree and on both branches after the onset of sexual maturity. (E) The tree is linear with specimens of both taxa interspersed with each other, but identical individual variations are unambiguously optimized in several specimens of one taxon and not along the main axis or in specimens of the other taxon; in this case, two groups are recovered and they may represent two taxa or sexual dimorphism. (F) If *T. kansasensis* and *T. nepaeolicus* represent opposite sexes of the same taxon, the tree will bifurcate with specimens of *T. kansasensis* on one branch, *T. nepaeolicus* on the other branch, and a mix of specimens near the root. (G) If *T. kansasensis* and *T. nepaeolicus* represent two different taxa, the tree will bifurcate at or near the root with all the *T. kansasensis* specimens on one branch and all the *T. nepaeolicus* specimens on the other; this

could also represent sexual dimorphism with an oversampling of adults in which specimens of *T. kansasensis* represent one sex and specimens of *T. nepaeolicus* represent the other.

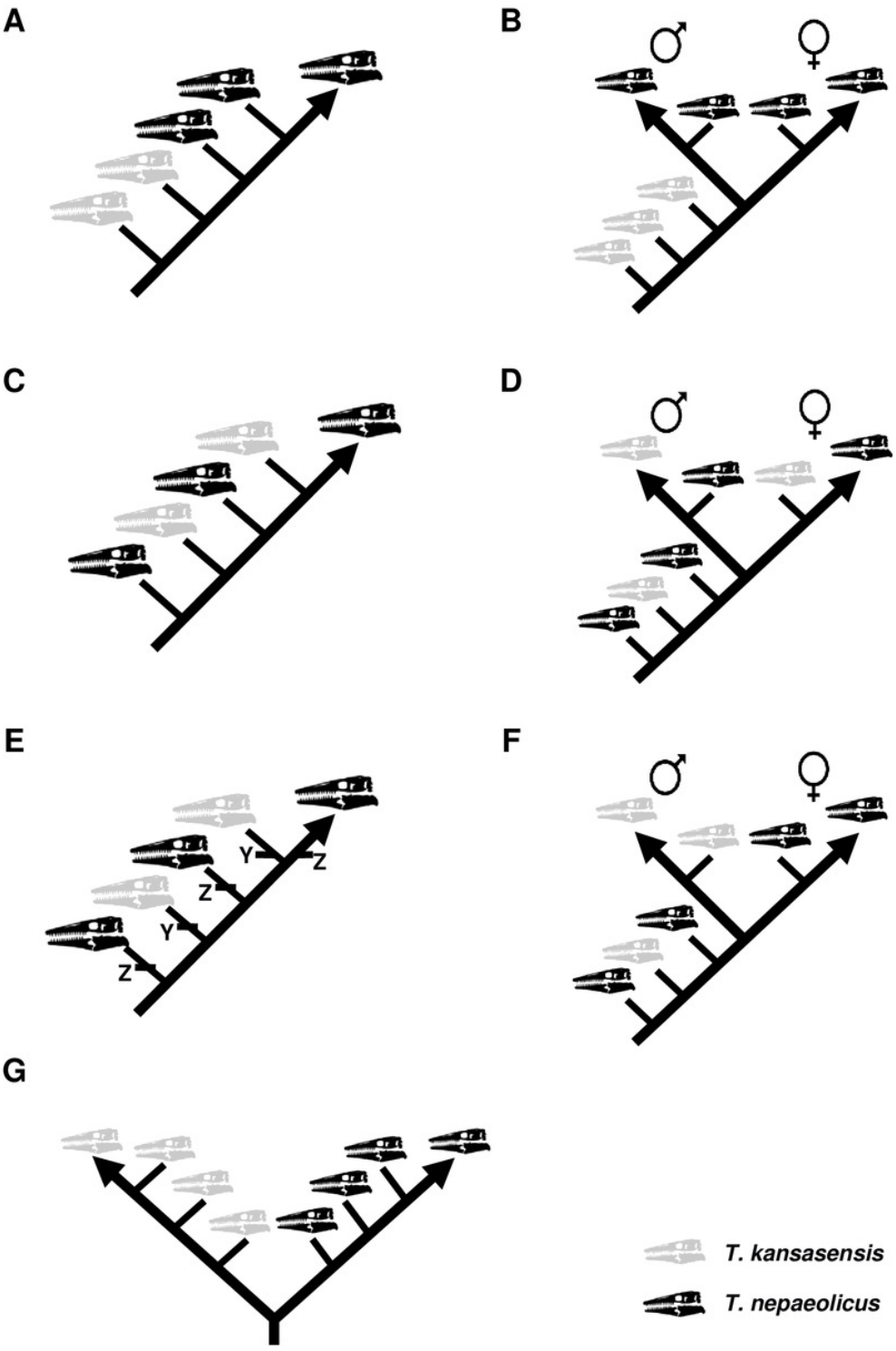
A
B
♂
♀
C
D
♂
♀
E
Y
Z
Z
Y
Z
F
♂
♀
G
T. kansasensis
T. nepaeolicus

Figure 6

Ontogram of one *Tylosaurus* sp. specimen and 22 *T. proriger* specimens based on a quantitative cladistic analysis.

The ontogram is a single tree and tree statistics are summarized in the upper left. Character states that define each growth stage are shown along the main branch, and the exemplar specimens are to the left of the main branch; the most mature individual, identified by the analysis with an artificial adult, is indicated by an arrow. The encircled numbers on the nodes are the growth stages, and the numbers to the right of them are the bootstrap and jackknife values, respectively (1000 replicates, <50% not shown). Unambiguous character reversals are shown in red. Individual variations that are unambiguously optimized are listed in Table S2. The ontogram supports the assignment of all specimens to *T. proriger* and does not show evidence of sexual dimorphism. Notes: specimen photographs are not to scale; FHSM VP 14845 is a neonate referable to *Tylosaurus* sp.; the photograph of KUVP 1032 has been inverted to face left.

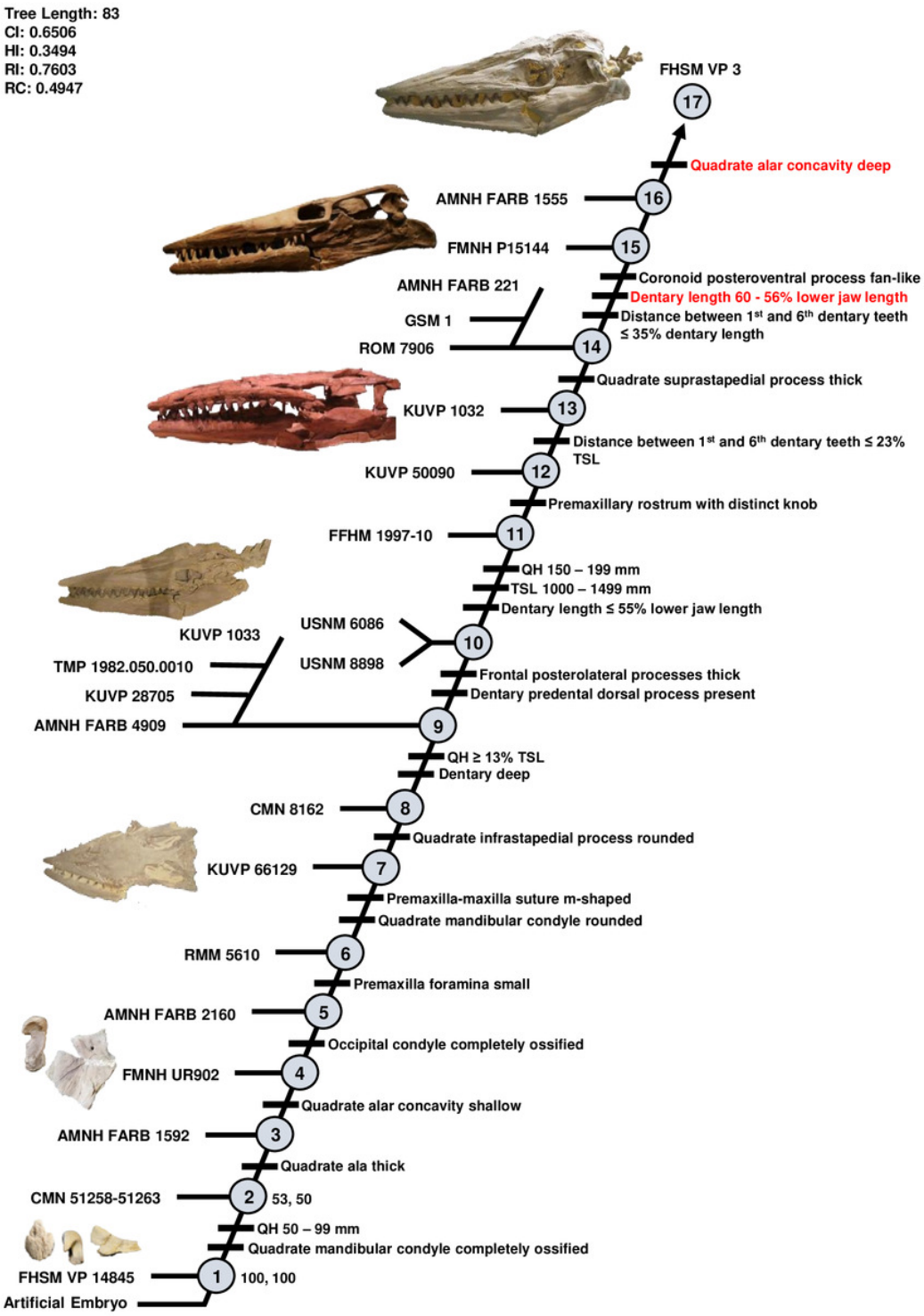
Tree Length: 83
CI: 0.6506
HI: 0.3494
RI: 0.7603
RC: 0.4947
FHSM VP 3
17
Quadrate alar concavity deep
AMNH FARB 1555
16
FMNH P15144
15
Coronoid posteroventral process fan-like
Dentary length 60 - 56% lower jaw length
Distance between 1st and 6th dentary teeth ≤ 35% dentary length
AMNH FARB 221
GSM 1
ROM 7906
14
Quadrate suprastapedial process thick
KUVP 1032
13
Distance between 1st and 6th dentary teeth ≤ 23% TSL
KUVP 50090
12
Premaxillary rostrum with distinct knob
FFHM 1997-10
11
QH 150 – 199 mm
TSL 1000 – 1499 mm
Dentary length ≤ 55% lower jaw length
KUVP 1033
USNM 6086
USNM 8898
10
TMP 1982.050.0010
KUVP 28705
AMNH FARB 4909
Frontal posterolateral processes thick
Dentary predental dorsal process present
9
QH ≥ 13% TSL
Dentary deep
CMN 8162
8
Quadrate infrastapedial process rounded
KUVP 66129
7
Premaxilla-maxilla suture m-shaped
Quadrate mandibular condyle rounded
RMM 5610
6
Premaxilla foramina small
AMNH FARB 2160
5
Occipital condyle completely ossified
FMNH UR902
4
Quadrate alar concavity shallow
AMNH FARB 1592
3
Quadrate ala thick
CMN 51258-51263
2
53, 50
QH 50 – 99 mm
Quadrate mandibular condyle completely ossified
FHSM VP 14845
Artificial Embryo
1
100, 100

Figure 7

Ontogram of one *Tylosaurus* sp. specimen, 11 *T. kansasensis* specimens, and seven *T. nepaeolicus* specimens based on a quantitative cladistic analysis.

Specimens identified as *T. nepaeolicus* are shown in blue; the type specimen of each taxon is indicated by an asterisk. The ontogram is a single tree and tree statistics are summarized in the upper left. Character states that define each growth stage are shown along the main branch, and the exemplar specimens are to the left of the main branch; the most mature individuals, identified by the analysis with an artificial adult, are indicated by arrows. The encircled numbers on the nodes are the growth stages, and the numbers to the right of them are the bootstrap and jackknife values, respectively (1000 replicates, <50% not shown). Unambiguous character reversals are shown in red. Individual variations that are unambiguously optimized are listed in Table S2. The ontogram does not bifurcate and thus supports synonymy of *T. kansasensis* with *T. nepaeolicus* and that *T. kansasensis* represent juveniles of *T. nepaeolicus* (Jiménez-Huidobro, Simões, and Caldwell, 2016), and does not show evidence for sexual dimorphism. Note: specimen photographs are not to scale; FHSM VP 14845 is a neonate referable to *Tylosaurus* sp.; the photographs of FGM V 43, FHSM VP 2209, and FHSM VP 78 have been inverted to face left.

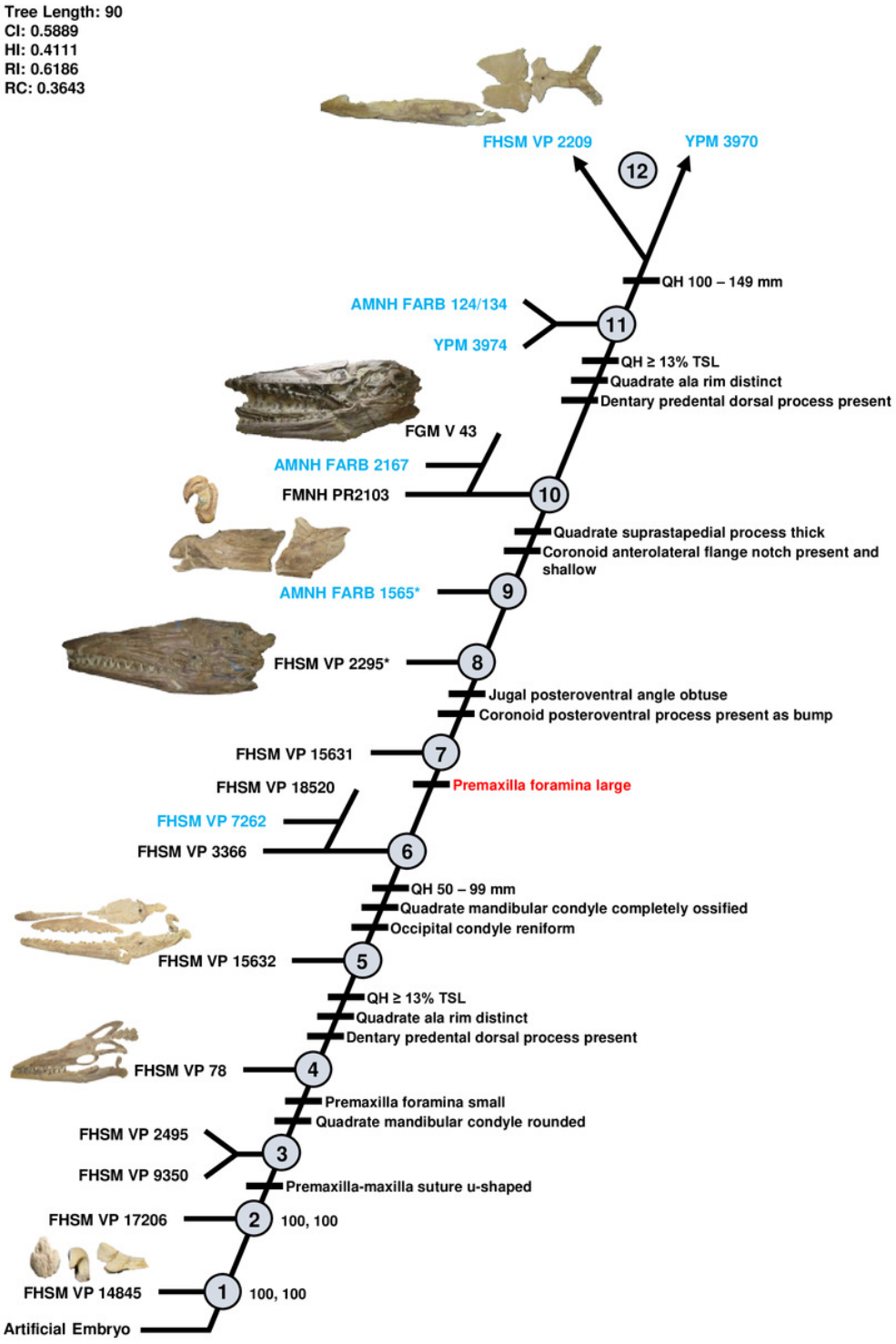
Tree Length: 90
CI: 0.5889
HI: 0.4111
RI: 0.6186
RC: 0.3643
FHSM VP 2209
YPM 3970
12
QH 100 – 149 mm
AMNH FARB 124/134
YPM 3974
11
QH ≥ 13% TSL
Quadrate ala rim distinct
Dentary predental dorsal process present
FGM V 43
AMNH FARB 2167
FMNH PR2103
10
Quadrate suprastapedial process thick
Coronoid anterolateral flange notch present and shallow
AMNH FARB 1565*
9
FHSM VP 2295*
8
Jugal posteroventral angle obtuse
Coronoid posteroventral process present as bump
FHSM VP 15631
7
FHSM VP 18520
Premaxilla foramina large
FHSM VP 7262
FHSM VP 3366
6
QH 50 – 99 mm
Quadrate mandibular condyle completely ossified
Occipital condyle reniform
FHSM VP 15632
5
QH ≥ 13% TSL
Quadrate ala rim distinct
Dentary predental dorsal process present
FHSM VP 78
4
Premaxilla foramina small
Quadrate mandibular condyle rounded
FHSM VP 2495
FHSM VP 9350
3
Premaxilla-maxilla suture u-shaped
FHSM VP 17206
2
100, 100
FHSM VP 14845
1
100, 100
Artificial Embryo

Figure 8

Ontogram of 30 *Tylosaurus* specimens (*Tylosaurus* sp., *T. kansasensis*, *T. nepaeolicus*, and *T. proriger*) based on a quantitative cladistic analysis to test for anagenesis in WIS *Tylosaurus* species.

The ontogram is based on a strict consensus of two trees, each with a length of 148 steps, a CI of 0.41, an HI of 0.59, an RI of 0.60, and an RC of 0.24. Holotypes are indicated by asterisks. Character states that define each growth stage are shown along the main branch, and the exemplar specimens are to the left of the main branch; the most mature individual, identified by the analysis with an artificial adult, is indicated by an arrow. The encircled numbers on the nodes are the growth stages, and the numbers below and to the right of them are the bootstrap and jackknife values, respectively (1000 replicates, <50% not shown). Unambiguous character reversals are shown in red. Specimens which are recovered as juveniles and subadults in the individual analyses were also recovered as immature in this analysis. Because all adult *T. proriger* specimens are recovered as more mature than all *T. nepaeolicus*, the hypothesis of anagenesis in WIS *Tylosaurus* is supported; additionally, all *T. nepaeolicus* specimens (except for the holotype) are recovered as more mature than all specimens of *T. kansasensis*, supporting the hypothesis that *T. kansasensis* are juveniles (Jiménez-Huidobro, Simões, and Caldwell, 2016). Abbreviations: **cr**, coronoid; **d**, dentary; **DL**, dentary length; **eccp**, ectopterygoid process of the pterygoid; **f**, frontal; **isp**, infrastapedial process of the quadrate; **p**, parietal; **pm**, premaxilla; **q**, quadrate; **ssp**, suprastapedial process of the quadrate. Note: in the individual analyses, “juvenile” specimens were recovered in the lower fourth of the tree, “subadults” were recovered in the second fourth of the tree, and “adult” specimens were recovered in the upper half of the tree.

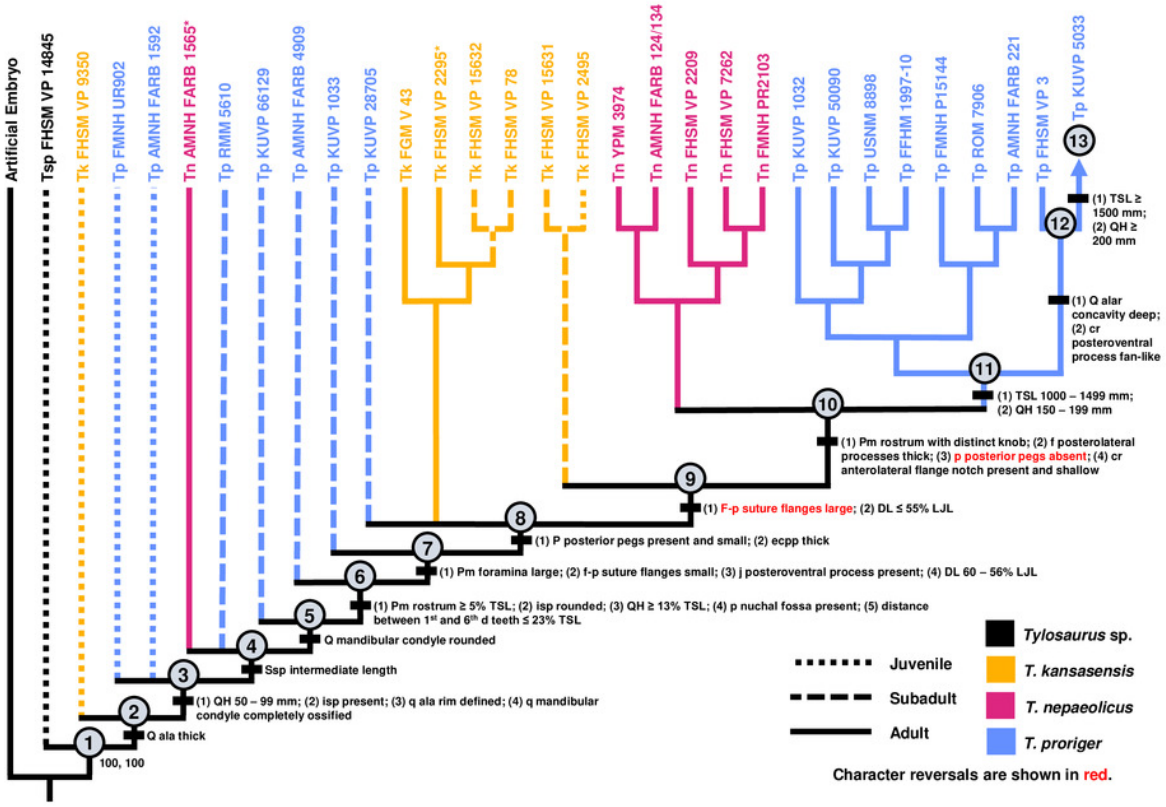
Artificial Embryo
Tsp FHSM VP 14845
Tk FHSM VP 9350
Tp FMNH UR902
Tp AMNH FARB 1592
Tn AMNH FARB 1565*
Tp RMM 5610
Tp KUVP 66129
Tp AMNH FARB 4909
Tp KUVP 1033
Tp KUVP 28705
Tk FGM V 43
Tk FHSM VP 2295*
Tk FHSM VP 15632
Tk FHSM VP 78
Tk FHSM VP 15631
Tk FHSM VP 2495
Tn YPM 3974
Tn AMNH FARB 124/134
Tn FHSM VP 2209
Tn FHSM VP 7262
Tn FMNH PR2103
Tp KUVP 1032
Tp KUVP 50090
Tp USNM 8898
Tp FFHM 1997-10
Tp FMNH P15144
Tp ROM 7906
Tp AMNH FARB 221
Tp FHSM VP 3
Tp KUVP 5033
1
100, 100
2
Q ala thick
3
(1) QH 50 – 99 mm; (2) isp present; (3) q ala rim defined; (4) q mandibular condyle completely ossified
4
Ssp intermediate length
5
Q mandibular condyle rounded
6
(1) Pm rostrum ≥ 5% TSL; (2) isp rounded; (3) QH ≥ 13% TSL; (4) p nuchal fossa present; (5) distance between 1st and 6th d teeth ≤ 23% TSL
7
(1) Pm foramina large; (2) f-p suture flanges small; (3) j posteroventral process present; (4) DL 60 – 56% LJL
8
(1) P posterior pegs present and small; (2) ecpp thick
9
(1) F-p suture flanges large; (2) DL ≤ 55% LJL
10
(1) Pm rostrum with distinct knob; (2) f posterolateral processes thick; (3) p posterior pegs absent; (4) cr anterolateral flange notch present and shallow
11
(1) TSL 1000 – 1499 mm; (2) QH 150 – 199 mm
12
(1) Q alar concavity deep; (2) cr posteroventral process fan-like
13
(1) TSL ≥ 1500 mm; (2) QH ≥ 200 mm
Juvenile
Subadult
Adult
Tylosaurus sp.
T. kansasensis
T. nepaeolicus
T. proriger
Character reversals are shown in red.

Figure 9

Ontogram of four *Te. nopcsai* specimens based on a quantitative cladistic analysis.

The ontogram is a single tree and tree statistics are summarized in the upper left. The type specimen is indicated by an asterisk. Character states that define each growth stage are shown along the main branch, and the exemplar specimens are to the left of the main branch; the most mature individual, identified by the highest number of growth changes, is indicated by an arrow. The encircled numbers on the nodes are the growth stages, and the numbers to the right of them are the bootstrap and jackknife values, respectively (1000 replicates, <50% not shown). The ontogram does not show evidence for sexual dimorphism. Individual variations that are unambiguously optimized are listed in Table S2.

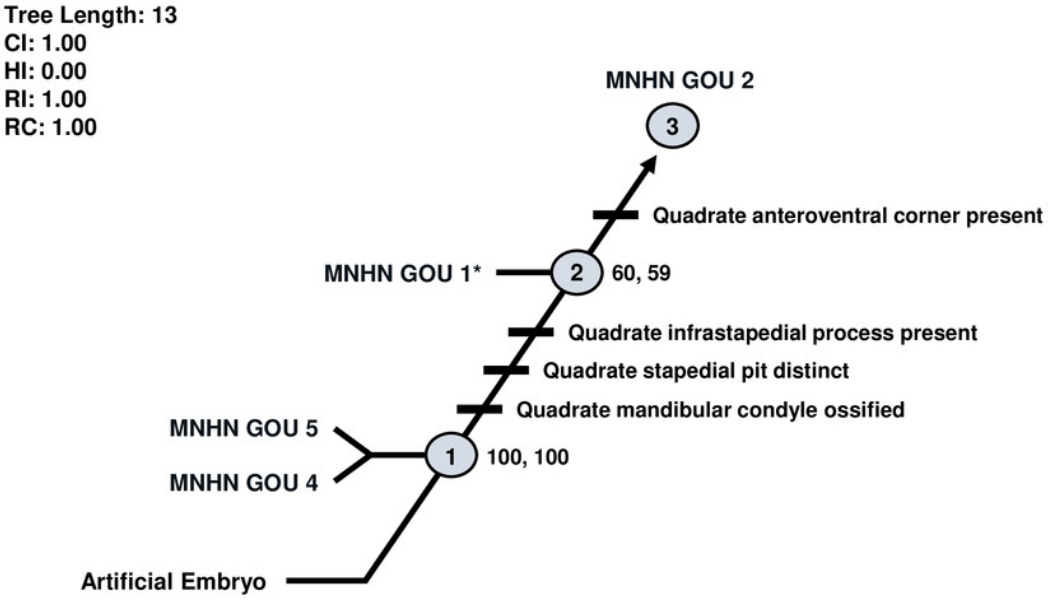
Tree Length: 13
CI: 1.00
HI: 0.00
RI: 1.00
RC: 1.00
MNHN GOU 2
3
Quadrate anteroventral corner present
MNHN GOU 1*
2
60, 59
Quadrate infrastapedial process present
Quadrate stapedial pit distinct
Quadrate mandibular condyle ossified
MNHN GOU 5
MNHN GOU 4
1
100, 100
Artificial Embryo

Figure 10

Figure 10: Ontogram of nine *M. hoffmannii* specimens based on a quantitative cladistic analysis.

The ontogram is a single tree and tree statistics are summarized in the upper left. The holotype is indicated by as asterisk. Character states that define each growth stage are shown along the main branch, and the exemplar specimens are to the left of the main branch; the most mature individual, identified by the highest number of growth changes, is indicated by an arrow. The encircled numbers on the nodes are the growth stages, and the numbers to the right of them are the bootstrap and jackknife values, respectively (1000 replicates, <50% not shown). Individual variations that are unambiguously optimized are listed in Table S2.

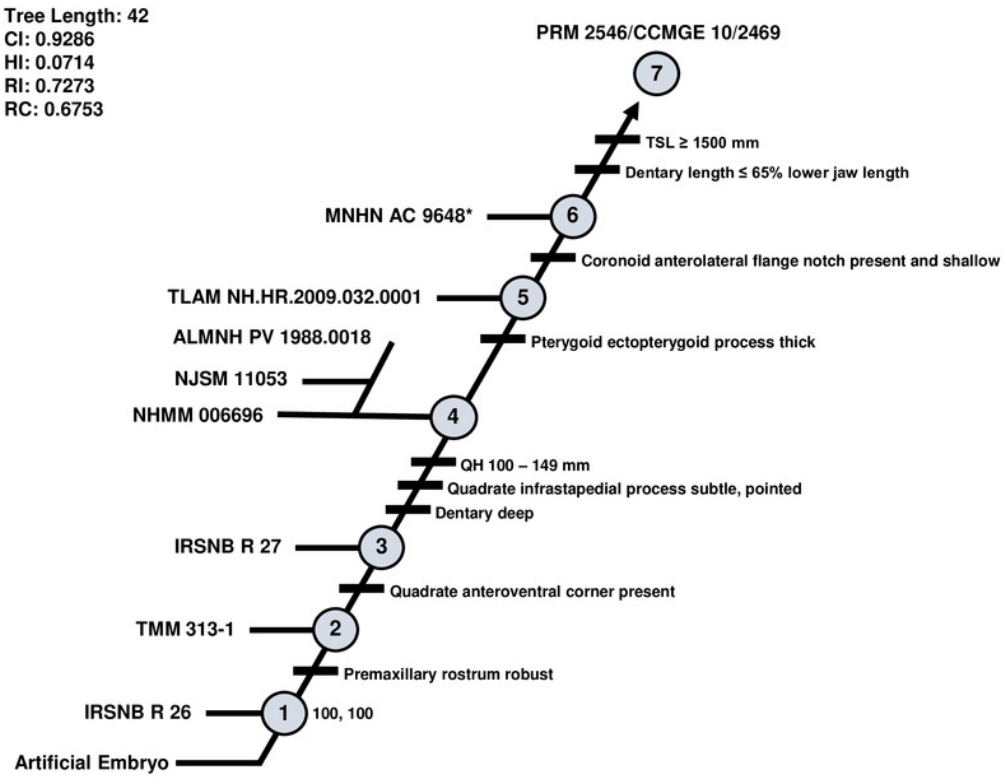
Tree Length: 42
CI: 0.9286
HI: 0.0714
RI: 0.7273
RC: 0.6753
PRM 2546/CCMGE 10/2469
7
TSL ≥ 1500 mm
Dentary length ≤ 65% lower jaw length
MNHN AC 9648*
6
Coronoid anterolateral flange notch present and shallow
TLAM NH.HR.2009.032.0001
5
ALMNH PV 1988.0018
Pterygoid ectopterygoid process thick
NJSM 11053
NHMM 006696
4
QH 100 – 149 mm
Quadrate infrastapedial process subtle, pointed
Dentary deep
IRSNB R 27
3
Quadrate anteroventral corner present
TMM 313-1
2
Premaxillary rostrum robust
IRSNB R 26
1
100, 100
Artificial Embryo

Figure 11

Size and maturity are positively correlated in *T. proriger*.

(A) Scatterplot and statistics for TSL data. (B) Scatterplot and statistics for QH data. The growth stages and size data for TSL and QH of each *T. proriger* specimen included in the growth series (for which measurements were available) were converted into ranks and plotted. Congruence between size rank and growth stage rank was tested with Spearman rank-order correlation. Both TSL and QH have a significant positive correlation with growth stage in this taxon. Shapiro-Wilk tests determined that growth rank, size rank, and raw measurement data are normally distributed.

A

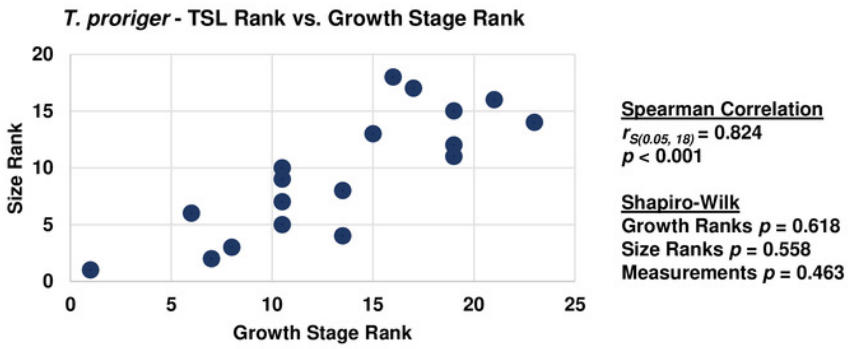
T. proriger - TSL Rank vs. Growth Stage Rank
Size Rank
Growth Stage Rank
0
5
10
15
20
25
Spearman Correlation
$r_{S(0.05, 18)}$ = 0.824
p < 0.001
Shapiro-Wilk
Growth Ranks p = 0.618
Size Ranks p = 0.558
Measurements p = 0.463

B

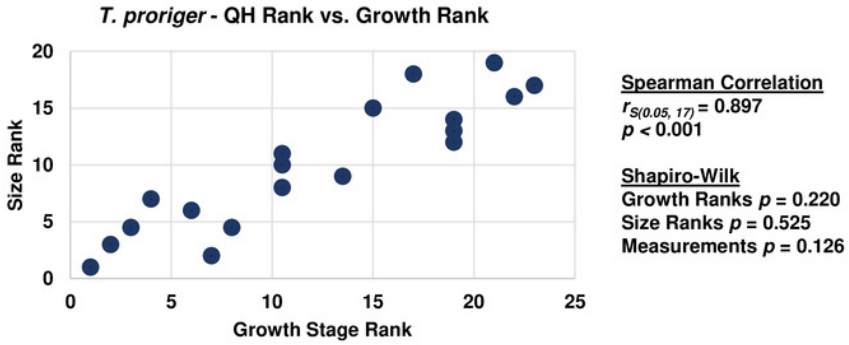
T. proriger - QH Rank vs. Growth Rank
Size Rank
Growth Stage Rank
0
5
10
15
20
25
Spearman Correlation
$r_{S(0.05, 17)}$ = 0.897
p < 0.001
Shapiro-Wilk
Growth Ranks p = 0.220
Size Ranks p = 0.525
Measurements p = 0.126

Figure 12

Size and maturity are positively correlated in *T. nepaeolicus*.

(A) Scatterplot and statistics for TSL data. (B) Scatterplot and statistics for QH data. The growth stages and size data for TSL and QH of each *T. nepaeolicus* specimen included in the growth series (for which measurements were available) were converted into ranks and plotted. Congruence between size rank and growth stage rank was tested with Spearman rank-order correlation. Both TSL and QH have a significant positive correlation with growth stage in this taxon. Shapiro-Wilk tests determined that TSL (but not QH) growth rank, size rank, and raw measurement data are normally distributed.

A

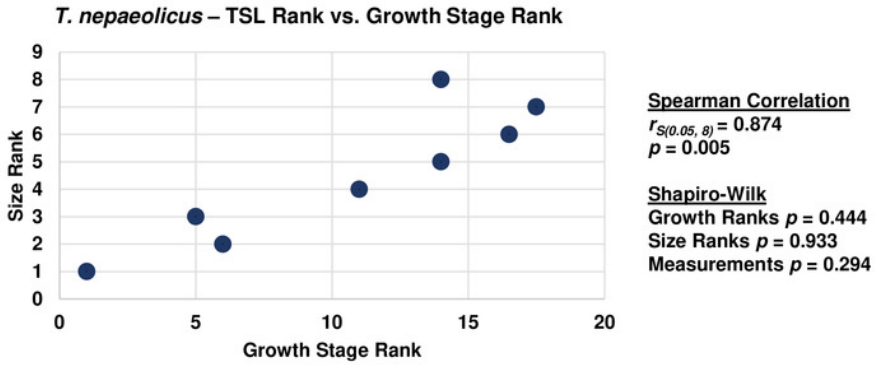
T. nepaeolicus – TSL Rank vs. Growth Stage Rank
Size Rank
Growth Stage Rank
0
1
2
3
4
5
6
7
8
9
0
5
10
15
20
Spearman Correlation
$r_{S(0.05, 8)}$ = 0.874
p = 0.005
Shapiro-Wilk
Growth Ranks p = 0.444
Size Ranks p = 0.933
Measurements p = 0.294

B

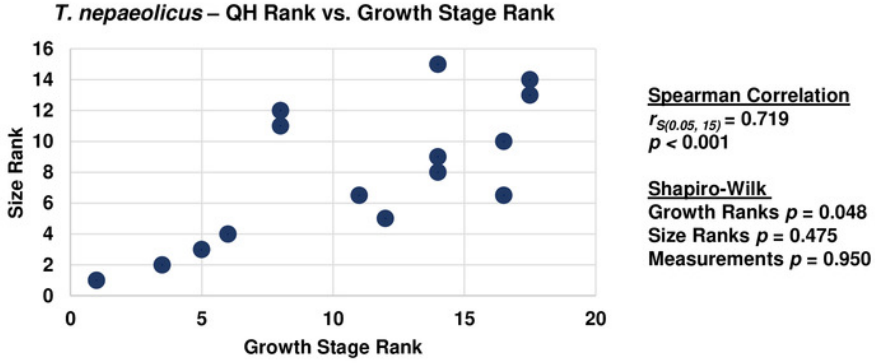
T. nepaeolicus – QH Rank vs. Growth Stage Rank
Size Rank
Growth Stage Rank
0
2
4
6
8
10
12
14
16
0
5
10
15
20
Spearman Correlation
$r_{S(0.05, 15)}$ = 0.719
p < 0.001
Shapiro-Wilk
Growth Ranks p = 0.048
Size Ranks p = 0.475
Measurements p = 0.950

Figure 13

Size and maturity are positively correlated in WIS *Tylosaurus* species.

(A) Scatterplot and statistics for TSL data. (B) Scatterplot and statistics for QH data. The growth stages and size data for TSL and QH of each specimen (for which measurements were available) included in the growth series including all three *Tylosaurus* taxa were converted into ranks and plotted. Congruence between size rank and growth stage rank was tested with Spearman rank-order correlation. Both TSL and QH have a significant positive correlation with growth stage. Shapiro-Wilk tests determined that growth rank, size rank, and raw measurement data are normally distributed.

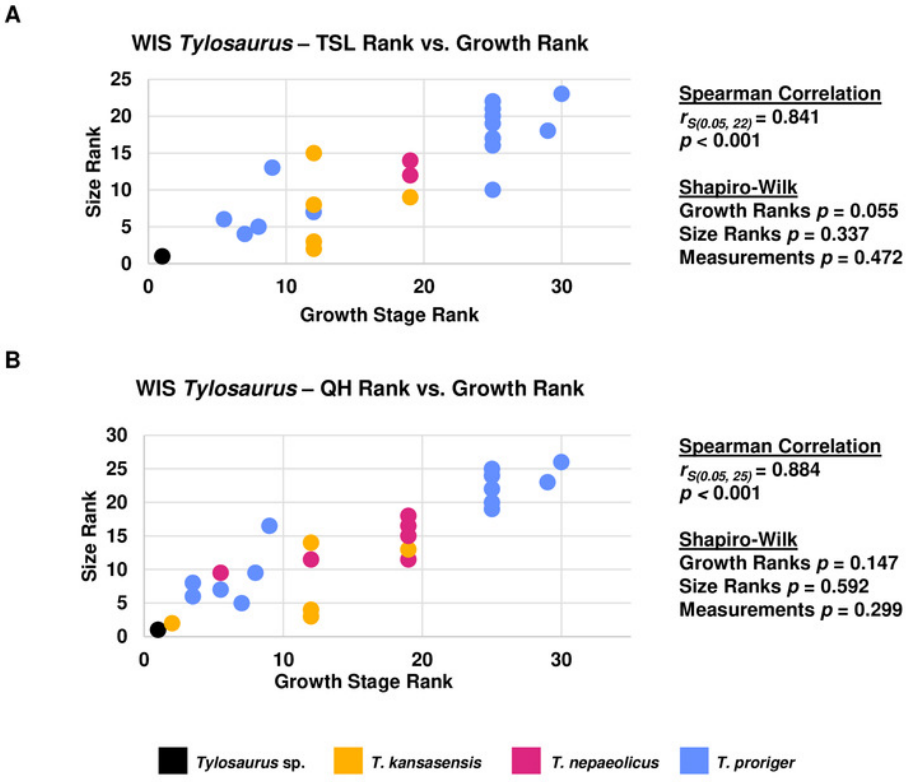
A
WIS Tylosaurus – TSL Rank vs. Growth Rank
Size Rank
Growth Stage Rank
0
5
10
15
20
25
0
10
20
30
Spearman Correlation
$r_{S(0.05, 22)}$ = 0.841
p < 0.001
Shapiro-Wilk
Growth Ranks p = 0.055
Size Ranks p = 0.337
Measurements p = 0.472
B
WIS Tylosaurus – QH Rank vs. Growth Rank
Size Rank
Growth Stage Rank
0
5
10
15
20
25
30
0
10
20
30
Spearman Correlation
$r_{S(0.05, 25)}$ = 0.884
p < 0.001
Shapiro-Wilk
Growth Ranks p = 0.147
Size Ranks p = 0.592
Measurements p = 0.299
Tylosaurus sp.
T. kansasensis
T. nepaeolicus
T. proriger

Figure 14

Size and maturity are positively correlated in *Te. nopcsai*.

(A) Scatterplot and statistics for TSL data. (B) Scatterplot and statistics for QH data. The growth stages and size data for TSL and QH of each *Te. nopcsai* specimen included in the growth series (for which measurements were available) were converted into ranks and plotted. Congruence between size rank and growth stage rank was tested with Spearman rank-order correlation. Both TSL and QH have a significant positive correlation with growth stage in this taxon, but this is likely due to the small sample size. Given the small number of individuals with size data available (n = 2), Shapiro-Wilk tests of normality were not possible.

A

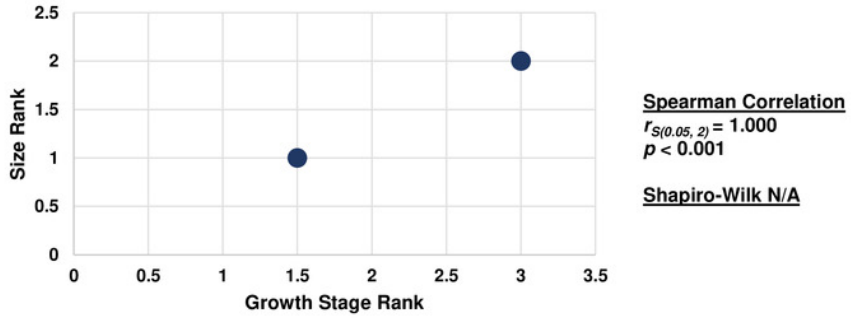
Te. nopcsai – TSL Rank vs. Growth Stage Rank
Size Rank
Growth Stage Rank
0
0.5
1
1.5
2
2.5
3
3.5
Spearman Correlation
$r_{S(0.05, 2)}$ = 1.000
p < 0.001
Shapiro-Wilk N/A

B

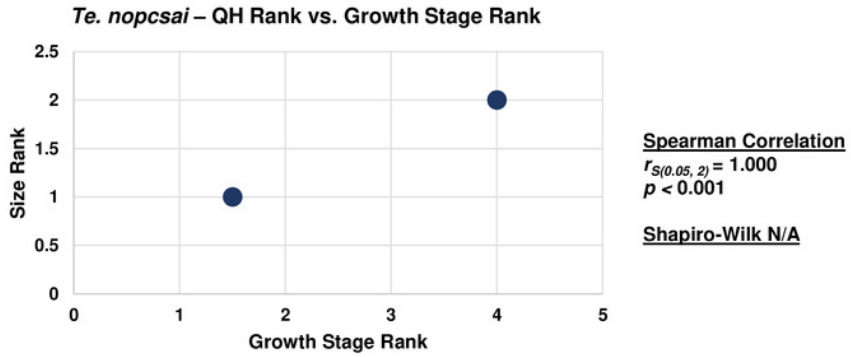
Te. nopcsai – QH Rank vs. Growth Stage Rank
Size Rank
Growth Stage Rank
0
0.5
1
1.5
2
2.5
3
4
5
Spearman Correlation
$r_{S(0.05, 2)}$ = 1.000
p < 0.001
Shapiro-Wilk N/A

Figure 15

Size and maturity are not significantly correlated in *M. hoffmannii*.

(A) Scatterplot and statistics for TSL data. (B) Scatterplot and statistics for QH data. The growth stages and size data for TSL and QH of each *M. hoffmannii* specimen included in the growth series (for which measurements were available) were converted into ranks and plotted. Congruence between size rank and growth stage rank was tested with Spearman rank-order correlation. Neither TSL nor QH have a significant correlation with growth stage in this taxon. Shapiro-Wilk tests determined that growth rank, size rank, and raw measurement data are normally distributed.

A

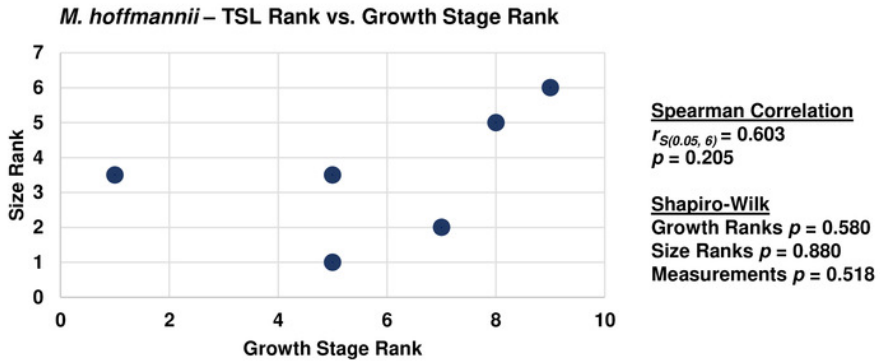
M. hoffmannii – TSL Rank vs. Growth Stage Rank
Size Rank
Growth Stage Rank
0
1
2
3
4
5
6
7
0
2
4
6
8
10
Spearman Correlation
$r_{S(0.05, 6)}$ = 0.603
p = 0.205
Shapiro-Wilk
Growth Ranks p = 0.580
Size Ranks p = 0.880
Measurements p = 0.518

B

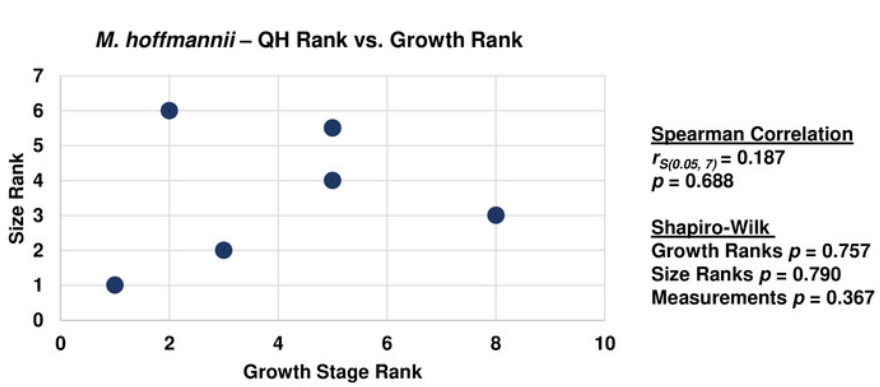
M. hoffmannii – QH Rank vs. Growth Rank
Size Rank
Growth Stage Rank
0
1
2
3
4
5
6
7
0
2
4
6
8
10
Spearman Correlation
$r_{S(0.05, 7)}$ = 0.187
p = 0.688
Shapiro-Wilk
Growth Ranks p = 0.757
Size Ranks p = 0.790
Measurements p = 0.367

Figure 16

Quadrate growth in WIS *Tylosaurus*.

Growth series of *Tylosaurus* sp. (A), *T. proriger* (B – F) and *T. nepaeolicus* (G – L) quadrates. (A) FHSM VP 14845. (B) FMNH UR902. (C) AMNH FARB 4909. (D) AMNH FARB 1555. (E) FHSM VP 3. (F) KUVP 5033. (G) FHSM VP 9350. (H) FHSM VP 15632. (I) FHSM VP 2295. (J) FGM V 43. (K) AMNH FARB 124/134. (L) AMNH FARB 2167. Scale bars are 5 cm. Notes: the photographs of FMNH UR902, FHSM VP 15632, FGM V 43, and AMNH FARB 124/134 have been inverted to face left; KUVP 5033 is included in the analysis with all three *Tylosaurus* taxa, but not in the individual *T. proriger* ontogram; in the ontogram, AMNH FARB 2167 is recovered as less mature (stage 10) than AMNH FARB 124/134 (stage 11).


A
B
C
D
E
F
G
H
I
J
K
L

Figure 17

Simplified cladogram showing growth characters which were found to be shared across two or more taxa in this project.

The asterisk indicates a growth character that was not recovered in either species of *Tylosaurus*.

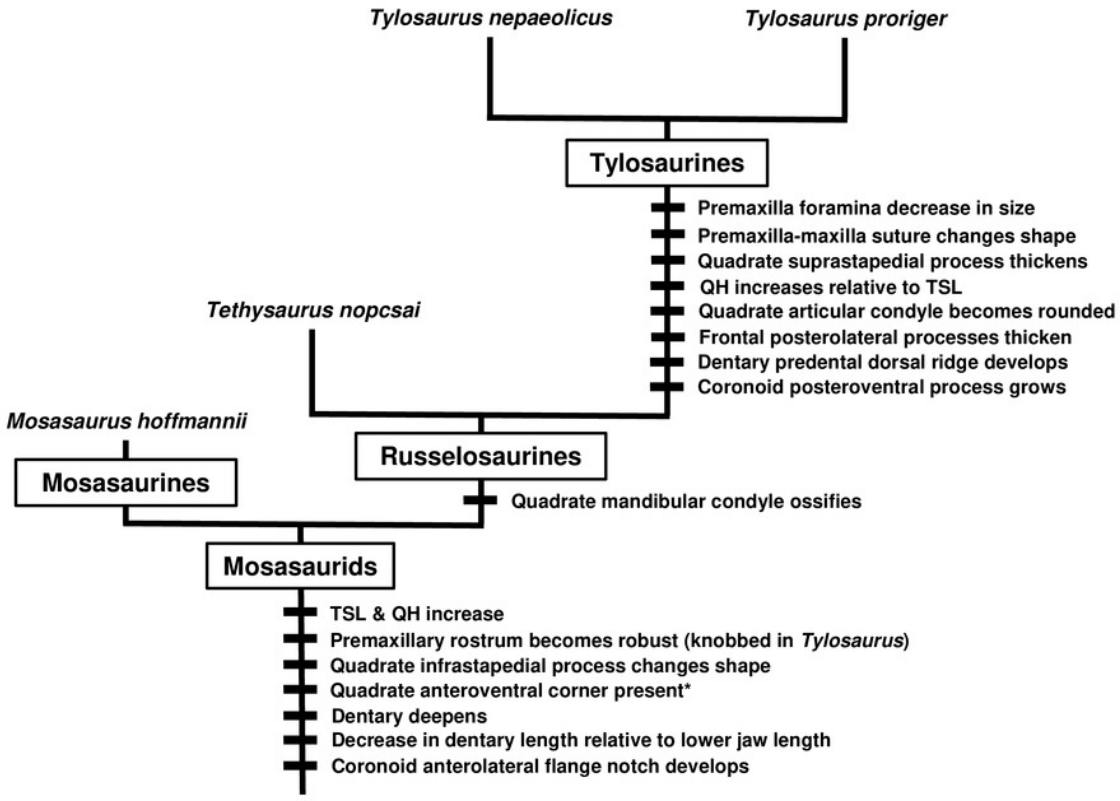

Table 1(on next page)

Measurements, in millimeters, of all specimens included in this project for which measurement data was available.

Measurements are rounded to the nearest whole millimeter. (A) Total skull length. (B) Premaxilla predental rostrum length. (C) Length between first and sixth maxillary teeth. (D) Quadrate height. (E) Lower jaw length. (F) Dentary length. (G) Dentary height. (H) Length between first and sixth dentary teeth. Measurement sources are listed in Table S1. Estimates made by the author using scale bars in the literature or due to incomplete material are indicated by a single asterisk, estimates from the literature are indicated by two asterisks, and missing measurements are indicated by question marks. Notes: TMP 1982.050.0010 is a cast of LACMNH 28964; CMN 51258 through 51263 are fragments from a single individual (Stewart and Mallon, 2018); AMNH FARB 124 and 134 are a skull and jaws, respectively, from a single individual (Jiménez-Huidobro and Caldwell, 2019); PRM 2546 is a cast of CCMGE 10/2469, and both were referenced for coding (Grigoriev, 2014); a measurement was published for (B) CMN 8162 (Stewart & Mallon, 2018), but it is inaccurate due to restoration of the specimen (T. Konishi, 2019, pers. comm.).

Specimen	A	B	C	D	E	F	G	H
***Tylosaurus* sp.**								
FHSM VP 14845	300**	3	?	30*	?	?	?	?
FHSM VP 14841	?	13	?	?	?	?	?	?
FHSM VP 14842	?	14	?	?	?	?	?	?
FHSM VP 14843	?	11	?	?	?	?	?	?
FHSM VP 14844	?	15	?	?	?	?	?	?
T. proriger								
RMM 5610	611**	21**	130**	72*	?	?	?	?
CMN 51258-51263	?	?	?	70*	?	?	?	?
CMN 8162	574	?	127	71	575	364	60*	172
KUVP 5033	1700*	87*	330*	225	1850*	900*	222*	315*
FHSM VP 3	1130	58	225	165	1228	694	152	218
FMNH P15144	1201	63	259	173	1343	761	84	239
AMNH FARB 221	1180*	?	?	135*	1132*	617*	87	?
AMNH FARB 4909	610	42	143	78	695	416	71	138
AMNH FARB 1555	?	?	?	152	?	?	?	?
USNM 6086	585	?	142	79	650	373	?	163
USNM 8898	710	40*	223	?	935	565	?	215
YPM 1268	?	?	141	78	?	?	?	130
YPM 3977	?	33	?	82	?	399	?	144
YPM 4002	?	36	234	?	?	?	?	220
YPM 3981	?	57	?	158	?	?	?	?
KUVP 1032	1212	57	268	170	1351	716	126*	260
AMNH FARB 1585	?	?	83	?	?	?	?	?
KUVP 66129	506	19	129	63	553	345*	47	120
FFHM 1997-10	1016	61	284	150	1220	667	?	251
TMP 1982.050.0010	810	46	186	111	872	543	?	174
FMNH UR902	?	?	?	75	?	?	?	?
FMNH UR820	?	54	?	?	?	?	?	?
GSM 1	980	62	241	133	1092	603	?	223
ROM 7906	1005	53	256	144	1245	?	?	235
AMNH FARB 2160	?	20	?	?	?	?	?	?
AMNH FARB 1560	?	41	?	?	?	?	?	?
AMNH FARB 1592	?	?	?	71	?	?	?	?
FHSM VP 6907	?	45	?	?	?	?	?	165
KUVP 1033	813	44	193	106	931	538	99	182
KUVP 50090	1300	49*	272*	?	1415*	780*	159	360*
KUVP 28705	615	31	138*	?	?	?	?	?
KUVP 65636	1180*	56	149	150	1200*	635	122	219
KUVP 1020	?	?	?	89	?	?	?	?
T. nepaeolicus								
AMNH FARB 1565	?	?	?	78	660	?	?	?
AMNH FARB 124/134	717	19	176	92	828	444	85	180
YPM 3980	?	?	181	110	?	?	?	?
YPM 3970	?	?	?	121	?	?	?	?
YPM 3969	?	25*	?	?	?	?	?	?
YPM 3974	?	23	139	82*	?	391	?	149
AMNH FARB 1561	?	41	?	?	?	?	?	?
FHSM VP 7262	?	44	175	106	?	585*	94	170
FHSM 2209	851*	44	201	133	1002	580	107	192
YPM 3979	?	10	85	?	?	236	?	83
YPM 3992	?	?	99	46	?	247	?	90
YPM 4000	?	28	?	68	?	355	?	135
YPM 3976	?	33	?	109	?	?	?	?

AMNH FARB 2167	?	?	?	155*	?	?	?	?
T. kansasensis								
FHSM VP 2295	650	27	154	82	724	404	72	130
FHSM VP 78	378	14	75	43	440	251	41	81
FHSM VP 2495	?	?	102	?	510	273	50	94
FHSM VP 3366	?	35	164	93	?	441	?	164
FHSM VP 9350	?	11	?	37	370	183	32	65
FHSM VP 13742	?	28*	?	?	980	509	95*	176
FHSM VP 14848	?	?	?	24	?	?	?	?
FHSM VP 15631	?	22	?	?	760	?	?	127*
FHSM VP 15632	360*	16*	82	45	414	240	39	71
FGM V 43	890	39	173	97	830	475	81	157
MCZ 1589	?	20	?	?	809**	460	?	?
YPM 40796	?	?	?	?	430**	240	?	?
LACMNH 127815	650**	?	?	?	730**	410	?	?
TMM 40092-27	?	14	?	?	?	?	?	?
TMM 81051-64	?	13	?	?	?	?	?	?
IPB R322	350*	?	75*	40*	410*	250*	?	?
FHSM VP 17206	?	26	?	?	?	?	?	?
FHSM VP 14840	?	13	?	?	?	?	?	?
FMNH PR2103	653	32	140*	87	723	415	84	134
FMNH UC1342	?	?	?	?	?	352	68	127
FHSM VP 18520	?	31	169	?	?	?	?	?
Te. nopcsai								
MNHN GOU 1	240*	n/a	39*	?	274*	160*	25*	40*
MNHN GOU 2	?	n/a	?	42*	?	?	?	?
MNHN GOU 3	?	n/a	?	?	?	?	?	?
MNHN GOU 4	100**	n/a	?	18**	?	?	?	?
MNHN GOU 5	?	n/a	?	?	?	?	?	?
M. hoffmannii								
NJSM 11053	1208	12*	298	190	1230	818	200*	270
NJSM 11052	?	?	?	190*	?	?	190*	?
AMNH FARB 1389	?	?	?	180*	?	?	?	?
ALMNH PV 1988.0018	?	?	?	190*	?	?	?	?
TMM 313-1	?	?	?	200*	?	?	?	?
YPM 773	?	?	?	200	?	?	?	?
TLAM NH.HR.2009.032.0001	1300*	?	?	?	?	840*	?	?
IRSNB R 27	?	?	?	140*	?	400*	60*	130*
MNHN AC 9648	1450*	?	350*	175*	1500*	1050*	150*	300*
IRSNB R 12	880*	15*	300*	?	1110*	675*	130*	270*
NHMM 006696	1440**	20*	?	183*	?	?	?	?
PRM 2546/CCMGE 10/2469	1700**	?	?	?	1800*	1020*	200*	350*
IRSNB R 26	1440*	?	330*	125*	1500*	1020*	130*	300*

1

Table 2(on next page)

Known tooth counts of specimens included in this project.

Missing counts are indicated by question marks. If tooth counts were available for both left and right bones, the number of teeth on the left bone is listed first.

Specimen	Maxillary Teeth	Dentary Teeth	Pterygoid Teeth
T. proriger			
CMN 8162	13	13	?
FHSM VP 3	13	13	?
FMNH P15144	13	14	10
AMNH FARB 4909	?	13	10
KUVP 1032	13	13	10
KUVP 66129	?	12	?
FFHM 1997-10	13	13	?
KUVP 1033	13	13	?
KUVP 28705	13	?	10
KUVP 65636	12	13	?
T. nepaeolicus			
AMNH FARB 124/134	13	14	8, 9
FHSM VP 7262	12	12	10, 9
FHSM VP 2209	13	14	?
T. kansasensis			
FHSM VP 2295	13	13	?
FHSM VP 78	?	12	?
FHSM VP 2495	?	13	?
FHSM VP 3366	?	11 - 12	?
FHSM VP 9350	?	13	?
FHSM VP 13742	?	13	?
FHSM VP 15632	12	15, 13	≥ 11
FGM V 43	13	13, 12	8
IPB R322	12	?	?
FMNH PR2103	13	10, 12	13, 11
FMNH UC1342	?	13	?
Te. nopcsai			
MNHN GOU 1	19 - 20	≥ 19	15 - 19
MNHN GOU 4	?	?	11
MNHN GOU 5	?	?	9
M. hoffmannii			
NJSM 11053	16	14	?
TMM 313-1	?	15	?
TLAM NH.HR.2009.032.0001	14	13	?
IRSNB R 27	?	14	?
MNHN AC 9648	14	14	8
IRSNB R 12	14	15	8
PRM 2546/CCMGE 10/2469	?	≥ 15	?
IRSNB R 26	13	?	8

1

Table 3(on next page)

Completeness of coding of all specimens included in this project.

Single asterisks indicate specimens which were excluded from the analysis (i.e. wildcard specimens, specimens with incomplete or redundant coding) that produced the ontograms for each taxon, and double asterisks indicate specimens which were included in the single-taxon analyses but excluded from the test for anagenesis in *Tylosaurus*. Notes: KUVP 5033 was excluded from the analysis of growth in *T. proriger* but was included in the test of anagenesis; the following specimens were mentioned in the literature, but could not be coded for any characters: *T. proriger* YPM 3990 and *T. proriger* YPM 4002.

Specimen	Number of Characters Coded	% of Characters Coded
***Tylosaurus* sp.**		
FHSM VP 14845	16	27.1
***FHSM VP 14843**	4	6.8
***FHSM VP 14841**	3	5.1
***FHSM VP 14844**	3	5.1
***FHSM VP 14842**	2	3.4
T. proriger		
AMNH FARB 4909	44	74.6
FMNH P15144	43	72.9
FHSM VP 3	38	64.4
KUVP 1033	38	64.4
KUVP 1032	35	59.3
KUVP 66129	35	59.3
RMM 5610	32	54.2
***KUVP 65636**	31	52.5
FFHM 1997-10	31	52.5
****CMN 8162**	28	47.5
AMNH FARB 221	28	47.5
***KUVP 5033**	25	42.4
KUVP 28705	24	40.7
****USNM 6086**	22	37.3
FMNH UR902	19	32.2
***KUVP 1020**	17	28.8
****AMNH FARB 1555**	15	25.4
KUVP 50090	14	23.7
CMN 51258-51263	12	20.3
USNM 8898	12	20.3
AMNH FARB 1592	11	18.6
****TMP 1982.050.0010**	10	16.9
***AMNH FARB 1585**	9	15.3
****GSM 1**	9	15.3
ROM 7906	7	11.9
****AMNH FARB 2160**	6	10.2
***MCZ 4374**	4	6.8
***KUVP 1129**	4	6.8
***FMNH UR820**	4	6.8
***FHSM VP 6907**	4	6.8
***HMG 1288**	3	5.1
***AMNH FARB 1543**	2	3.4
***YPM 3977**	2	3.4
***AMNH FARB 1560**	2	3.4
***YPM 1268**	1	1.7
***YPM 3981**	1	1.7
***FHSM VP 2496**	1	1.7
T. nepaeolicus		
AMNH FARB 124/134	39	66.1
FHSM VP 2209	35	59.3
FHSM VP 7262	29	49.2
YPM 3974	17	28.8
AMNH FARB 1565	15	25.4
****AMNH FARB 2167**	13	22.0
***AMNH FARB 1561**	7	11.9
****YPM 3970**	6	10.2
***YPM 3969**	4	6.8

***YPM 3992**	2	3.4
***YPM 4000**	2	3.4
***YPM 3980**	1	1.7
***YPM 3979**	1	1.7
***YPM 3976**	1	1.7
T. kansasensis		
FHSM VP 2295	40	67.8
FMNH PR2103	40	67.8
FHSM VP 15632	38	64.4
FHSM VP 78	33	55.9
FGM V 43	31	52.5
FHSM VP 9350	26	44.1
****FHSM VP 3366**	24	40.7
FHSM VP 2495	18	30.5
FHSM VP 15631	15	25.4
***FHSM VP 13742**	13	22.0
****FHSM VP 18520**	13	22.0
***FHSM VP 14848**	12	20.3
***IPB R322**	9	15.3
****FHSM VP 17206**	4	6.8
***FMNH UC1342**	4	6.8
***FHSM VP 14840**	3	5.1
***MCZ 1589**	2	3.4
***LACMNH 127815**	2	3.4
***YPM 40796**	1	1.7
***TMM 40092-17**	1	1.7
***TMM 81051-64**	1	1.7
Te. nopcsai		
MNHN GOU 1	27	45.8
MNHN GOU 2	16	27.1
MNHN GOU 4	16	27.1
***MNHN GOU 3**	8	13.6
MNHN GOU 5	2	3.4
M. hoffmannii		
IRSNB R 26	31	52.5
MNHN AC 9648	28	47.5
NJSM 11053	26	44.1
IRSNB R 27	17	28.8
TLAM NH.HR.2009.032.001	16	27.1
***NJSM 11052**	14	23.7
TMM 313-1	14	23.7
***IRSNB R 12**	14	23.7
NHMM 006696	14	23.7
PRM 2546/CCMGE 10/2496	11	18.6
***AMNH FARB 1389**	10	16.9
ALMNH PV 1988.0018	10	16.9
***YPM 773**	9	15.3
***NHMUK 42929**	5	8.5
***TSMHN 11201**	4	6.8
***TSMHN 11376**	3	5.1
***NHMUK PV OR 11589**	2	3.4
***TSMHN 11202**	2	3.4
***TSMHN 11245**	2	3.4
***IRSNB R 24**	2	3.4
***YPM 430**	2	3.4

***IRSNB R 302**	1	1.7	

1

Table 4(on next page)

Growth ranks, size data, and size ranks used in the Spearman rank-order correlation tests in *T. proriger*.

Asterisks indicate estimates from the literature.

Specimen	Growth Rank	TSL (mm)	TSL Size Rank	QH (mm)	QH Size Rank
FHSM VP 14845	1	300*	1	30*	1
CMN 51258-51263	2	-	-	70*	3
AMNH FARB 1592	3	-	-	71	4.5
FMNH UR902	4	-	-	75	7
RMM 5610	6	611*	6	72*	6
KUVP 66129	7	506	2	63	2
CMN 8162	8	574	3	71	4.5
AMNH FARB 4909	10.5	610	5	78	8
TMP 1982.050.0010	10.5	810	9	111	11
KUVP 1033	10.5	813	10	106	10
KUVP 28705	10.5	615	7	-	-
USNM 6086	13.5	585	4	79	9
USNM 8898	13.5	710	8	-	-
FFHM 1997-10	15	1016	13	150	15
KUVP 50090	16	1300	18	-	-
KUVP 1032	17	1212	17	170	18
AMNH FARB 221	19	1180	15	135	13
GSM 1	19	980	11	133	12
ROM 7906	19	1005	12	144	14
FMNH P15144	21	1201	16	173	19
AMNH FARB 1555	22	-	-	151	16
FHSM VP 3	23	1130	14	165	17

1

Table 5(on next page)

Growth ranks, size data, and size ranks used in the Spearman rank-order correlation tests in *T. nepaeolicus*.

Single asterisks indicate estimates by the author, and double asterisks are estimates from the literature.

Specimen	Growth Rank	TSL (mm)	TSL Size Rank	QH (mm)	QH Size Rank
FHSM VP 14845	1	300**	1	30**	1
FHSM VP 9350	3.5	-	-	37	2
FHSM VP 78	5	378	5	43	3
FHSM VP 15632	6	360*	6	46	4
FHSM VP 7262	8	-	-	106	12
FHSM VP 3366	8	-	-	93	11
FHSM VP 2295	11	650	11	82	6.5
AMNH FARB 1565	12	-	-	78	5
AMNH FARB 2167	14	-	-	155	15
FGM V 43	14	890*	14	88	9
FMNH PR2103	14	653	14	87	8
YPM 3974	16.5	-	-	82**	6.5
AMNH FARB 124/134	16.5	717	16.5	92	10
YPM 3970	17.5	-	-	121	13
FHSM VP 2209	17.5	851*	11	133	14

1

Table 6(on next page)

Growth ranks, size data, and size ranks used in the Spearman rank-order correlation tests in the analysis including *Tylosaurus* sp. (Tsp), *T. kansasensis* (Tk), *T. nepaeolicus* (Tn), and *T. proriger* (Tp).

Single asterisks indicate estimates by the author, and double asterisks are estimates from the literature.

Specimen	Growth Rank	TSL (mm)	TSL Size Rank	QH (mm)	QH Size Rank
Tsp FHSM VP 14845	1	300**	1	30**	1
Tk FHSM VP 9350	2	-	-	37	2
Tp AMNH FARB 1592	3.5	-	-	71	6
Tp FMNH UR902	3.5	-	-	75	8
Tp RMM 5610	5.5	611**	6	72**	7
Tp AMNH FARB 1565	5.5	-	-	78	9.5
Tp KUVP 66129	7	506	4	63	5
Tp AMNH FARB 4909	8	610	5	78	9.5
Tp KUVP 1033	9	813	13	106	16.5
Tp KUVP 28705	12	615	7	-	-
Tk FHSM VP 78	12	378	3	43	3
Tk FHSM VP 15632	12	360*	2	46	4
Tk FHSM VP 2295	12	650	8	82	11.5
Tk FGM V 43	12	890*	15	88	14
Tn FHSM VP 7262	19	-	-	106	16.5
Tk FMNH PR2103	19	653	9	87	13
Tn YPM 3974	19	-	-	82**	11.5
Tn AMNH FARB 124/134	19	717	12	92	15
Tn FHSM VP 2209	19	851*	14	133	18
Tp USNM 8898	25	710	10	-	-
Tp ROM 7906	25	1005	16	144	20
Tp FFHM 1997-10	25	1016	17	150	22
Tp AMNH FARB 221	25	1180	19	135	19
Tp FMNH P15144	25	1201	20	173	25
Tp KUVP 1032	25	1212	21	170	24
Tp KUVP 50090	25	1300	22	-	-
Tp FHSM VP 3	29	1130	18	165	23
Tp KUVP 5033	30	1700*	23	225	26

1

Table 7 (on next page)

Growth ranks, size data, and size ranks used in the Spearman rank-order correlation tests in *Te. nopcsai*.

Single asterisks indicate estimates by the author, and double asterisks are estimates from the literature.

Specimen	Growth Rank	TSL (mm)	TSL Size Rank	QH (mm)	QH Size Rank
MNHN GOU 4	1.5	100**	1	18**	1
MNHN GOU 1	3	240*	2	-	-
MNHN GOU 2	4	-	-	42*	2

1

Table 8(on next page)

Growth ranks, size data, and size ranks used in the Spearman rank-order correlation tests in *M. hoffmannii*.

Single asterisks indicate estimates by the author, and double asterisks are estimates from the literature.

Specimen	Growth Rank	TSL (mm)	TSL Size Rank	QH (mm)	QH Size Rank
IRSNB R 26	1	1440*	3.5	125*	1
TMM 313-1	2	-	-	200*	6
IRSNB R 27	3	-	-	140*	2
NJSM 11053	5	1208	1	190	5.5
NHMM 006696	5	1440**	3.5	183*	4
ALMNH PV 1988.0018	5	-	-	190*	5.5
TLAM NH.HR.2009.032.0001	7	1300*	2	-	-
MNHN AC 9648	8	1450*	5	175*	3
PRM 2546/CCMGE 10/2469	9	1700**	6	-	-

1